공학박사 학위논문

Generation of charged nanoparticles via controlling the motion of post spark discharge dusty plasma

스파크 방전후의 플라즈마의 거동 조절을 통한

하전 나노입자의 발생

2017 년 2월

서울대학교 대학원

기계항공공학부

김 웅 식

This page is intended to be blank

Generation of charged nanoparticles via controlling the motion of post spark discharge dusty plasma

스파크 방전후의 플라즈마의 거동 조절을 통한

하전 나노입자의 발생

지도 교수 최 만 수

이 논문을 공학박사 학위논문으로 제출함

2016 년 12 월

서울대학교 대학원

기계항공공학부

김 웅 식

김웅식의 공학박사 학위논문을 인준함

2016 년 12 월

위 원 장	전 누 리	(인)
부위원장	최 만 수	(인)
위 원	고 승 환	(인)
위 원	이 정 훈	(인)
위 원	김 형 철	(인)

This page is intended to be blank

Generation of charged nanoparticles via controlling the motion of post spark discharge dusty plasma

Woongsik Kim
School of Mechanical and Aerospace Engineering
The Graduate School
Seoul National University

Abstract

The spark discharge method is a versatile method for generating nanoparticles in the gas phase. The method has been used to many research fields: nanoparticle synthesis, optic device, assembly of nanoparticles, etc. Although it has many advantages, there have been two challenges to be overcome such as preventing agglomeration and generating a large amount of charged particles. Many research groups have tried to overcome these challenges up to now. However, previous researches have limitation with respect to solving the two challenges by manipulating only the parameters of pre spark discharge procedure such as spark frequency, spark energy, gas flow rate, ion injection, etc. Though few researches have been carried out on controlling the post spark discharge regime, it is very important because it is possible to solve the challenges radically through the analysis of the mechanism on the post spark discharge regime.

In this work, a post spark discharge manipulator (PSDM), which could control the post spark regime with electric field, was designed and tested to prevent agglomeration and generate a large amount of charged particles. In addition, electric field effect in post spark discharge regime was studied and

the mechanism was suggested through the analysis of forces acting on the post spark dusty plasma.

We report a strong size-selective effect of the non-uniform external electric field on unitary charged nanoparticles in residual dusty plasma generated by spark discharge. It has been found that the field influences the outcome particle size distribution function considerably by expelling smaller particles out of the residual plasma cloud so that they cannot neutralize or agglomerate. Meantime larger particles being dragged by the plasma cloud neutralize and disappear at walls therefore the particle size distribution function shifts to small sizes. We give a simple theory explaining the field effect and not only suggest its application for a patterning technique, but also show the results.

Keywords: spark discharge, post spark discharge manipulator (PSDM), common spark discharge generator (CSDG), post spark residual dusty plasma, pre spark discharge, electric force, ion drag force, dipole parameter 'P';

Contents

List of Tables

Nomenclature

τ_p	Post spark plasma lifetime	[s]
V_d	Discharge voltage	[V]
T	Traveling time	[ms]
λ_D	Debye length of plasma	[cm]
F_E	Electric field force	[N]
F_{ion}	Ion drag force	[N]
Q_d	Particle charge	[C]
r_d	Particle radius	[nm]
n_i	Ion concentration	$[\#/cm^3]$
T_i	Ion temperature	[K]
v_i	Ion velocity	[m/s]
λ_p	Radius of plasma ball	[cm]
R	Distance between plasma ball and electrode	[cm]
d_p	particle diameter	[nm]
μ_i	Dynamical ion viscosity	$[\mathrm{g/cm \cdot s}]$
$\vec{d}$	Dipole moment of the plasma cloud	$[cm^2 \cdot N]$
V	Applying voltage on the electrode	[V]

e	charge of an electron	$[1.602\times10^{-19}\,\mathrm{C}]$
P	Dimensionless dipole parameter	

List of Figures

This page is intended to be blank

Chapter 1.
Introduction

1.1. Background of Research

Since the earliest accounts of electric discharges on smoke, fumes and suspended particles dating back to 1600 and of the experiments of clearing smoke in a jar by applying a high voltage to a corona wire electrode back to 1824 (see book '*Introduction to Complex Plasma*' and references therein) scientists have descended from macro-scale to nano-scale concerning the ways of manipulation of particles with electric field. Spark discharge has been known as the easiest way to generate unagglomerated nanoparticles in large quantities out of many pure materials like noble metals (Borra. 2006; Tabrizi et al. 2009; Han et al. 2012; Park et al. 2014). Many researchers in recent years have been interested on the spark discharge method; this is a facile and effective method for generating neutral and charged nanoparticles in the gas phase (Tabrizi et al., 2009). This method was developed by Schwyn et al (Schwyn et al., 1988). Since then, it has been studied by many research groups (Evans et al., 2003; Horvath and Gangl., 2003; Roth et al., 2004; Han et al., 2012; Park et al., 2014; Ha et al., 2014) due to its many merits.

Controlling the size of the nanoparticles (both charged and neutral) produced in the discharge is vitally needed for such applications as nano-electronics where small diameters and narrow particle size distribution function (PDF) are in demand (Kim et al. 2006; Lee et al. 2011; Ha et al. 2014; Choi et al. 2015). Well known parameters of size control in spark discharge are the spark energy, repetition frequency f and the residence time

(the gas flow rate) (Meuller et al. 2012). However in high gas flow rate condition, it is difficult to fabricate 3D nanoparticle structures since particles are dominated by inertia force rather than electrostatic force. In this condition, particles are easy to deviate electrostatic lens line (Lee at al., 2011). It is needed low gas flow rate condition to avoid this phenomenon. But this condition can give rise to agglomerate among the spark-generated particles (Park et al. 2014). Although many researchers have tried to overcome this agglomeration problem, previous researches have limitation with respect to controlling the agglomeration phenomenon by only the parameters of pre spark discharge procedure. The parameters of pre spark discharge procedure such as gap distance and the components of circuit cannot be varied during experiment and the change of parameter such as gas flow rate can have influence on another process of the experiment as well as size and amount of particles. It needs to investigate the parameters of post spark regime which can affect the size and amount of nanoparticles without varying the initial condition of spark, namely the pre spark discharge procedure. And the parameters of post spark regime have a potential to discover new method about increasing charged nanoparticles. A large amount of charged particles are needed to construct multi-dimensional nanoparticle structures in short time. However few researches have been carried out on discovering the parameters of post spark discharge regime. It is required fundamental research on the post spark discharge regime.

Motivated by these, in the present study, the new spark discharge

generator was developed, which is capable of preventing agglomeration and generating a large amount of charged particles by utilizing the electric field effect in the post spark regime.

And it was attempted to analyze the electric field effect to the particles in post spark dusty plasma in theoretically and experimentally in case of $t \lesssim \tau_p$, namely, the time before residual post spark plasma die.

1.2. Objectives for Research

In the present study, we developed the new spark discharge generator capable of preventing agglomeration and generating a large amount of charged particles by utilizing the electric field effect in the post spark regime. Furthermore, the analysis about forces acting on the post spark dusty (complex) plasma was achieved for finding the mechanism about post spark regime.

One may expect that charged nanoparticles generated within spark discharge (that lasts less than one microsecond[4]) and floating in the post-discharge plasma should also respond to non-uniform electric fields. However in spite of years of investigation none of such effects has been reported except for the case of patterning when the positively charged particles are guided by the conFigured electric fields long after residual post-spark plasma completely died at $t \gg \tau_p$ where τ_p is the post-spark plasma lifetime.

Therefore, it was attempted to analyze the electric field effect to the particles in post spark dusty plasma in theoretically and experimentally.

And we tried to eliminate large agglomerates and the size of particles was decreased, so well-patterned nanostructures were fabricated.

1.3. References

Biskos,G.,Vons,V.,Yurteri,C.,&Schmidt-Ott,A.(2008). Generation and sizing of particles for aerosol-based nanotechnology. *KONA PowderParticle Journal*, 26, 13–35.

Borra,J.-P.(2006). Nucleation and aerosol processing in atmospheric pressure electrical discharges: powders production, coatings and filtration. *JOURNAL OF PHYSICS D: APPLIED PHYSICS* 39, R19–R54.

Choi,H.,Kang,S.,Jung,W.,Jung,Y.,Park,S.,Kim,D.,&Choi,M.(2015). Controlled electrostatic focusing of charged aerosol nanoparticles via an electrified mask. *Journal of Aerosol Science*, 88, 90-97.

Evans,D.E.,Harrison,R.M.,&Ayres,J.G.(2003).The generation and characterisation of elemental carbon aerosols for human challenge studies. *Journal of Aerosol Science*, 34, 1023–1041.

Horvath,H.,&Gangl,M.(2003).A low-voltage spark generator for production of carbon particles. *Journal of Aerosol Science*, 34, 1581–1588.

Kim,H.,Kim,J.,Yang,H.,Suh,J.,Kim,T.,Han,B.,Kim,S.,Kim,D.,Pikhitsa, PV.,&Choi,M.(2006).Parallel patterning of nanoparticles via electrodynamic focusing of charged aerosols. Nature *Nanotechnology*, 1, 117–121.

Biskos,G.,Vons,V.,Yurteri,C.,&Schmidt-Ott,A.(2008). Generation and sizing of particles for aerosol-based nanotechnology. *KONA*

PowderParticle Journal, 26, 13–35.

Borra,J.-P.(2006). Nucleation and aerosol processing in atmospheric pressure electrical discharges: powders production, coatings and filtration. *JOURNAL OF PHYSICS D: APPLIED PHYSICS* 39, R19–R54.

Choi,H.,Kang,S.,Jung,W.,Jung,Y.,Park,S.,Kim,D.,&Choi,M.(2015). Controlled electrostatic focusing of charged aerosol nanoparticles via an electrified mask. *Journal of Aerosol Science*, 88, 90-97.

Evans,D.E.,Harrison,R.M.,&Ayres,J.G.(2003).The generation and characterisation of elemental carbon aerosols for human challenge studies. *Journal of Aerosol Science*, 34, 1023–1041.

Horvath,H.,&Gangl,M.(2003).A low-voltage spark generator for production of carbon particles. *Journal of Aerosol Science*, 34, 1581–1588.

Kim,H.,Kim,J.,Yang,H.,Suh,J.,Kim,T.,Han,B.,Kim,S.,Kim,D.,Pikhitsa, PV.,&Choi,M.(2006).Parallel patterning of nanoparticles via electrodynamic focusing of charged aerosols. Nature *Nanotechnology*, 1, 117–121.

Han, K., Kim, W., Yu, J., Lee, J., Lee, H., Gyu Woo, C., & Choi, M. (2012). A study of pin-to-plate type spark discharge generator for producing unagglomerated nanoaerosols. *Journal of Aerosol Science, 52*, 80-88. doi: 10.1016/j.jaerosci.2012.05.002

Chapter 2.

Generation of un-agglomerated charged nanoparticles and particle size selection effect via controlling the electric field in the post spark discharge regime

2.1. Introduction

Much research in recent years has been focused on the spark discharge method; this is a facile and effective method for generating neutral and charged nanoparticles in the gas phase (Tabrizi et al., 2009). The method was developed by Schwyn et al (Schwyn et al., 1988). Since then, it has been studied by many research groups (Evans et al., 2003; Horvath and Gangl., 2003; Roth et al., 2004; Han et al., 2012; Park et al., 2014; Ha et al., 2014) due to its many advantages.

The method can be applied to many kinds of conductive material including semi-conductors. It does not require expensive precursors and there is no melting point limitation (Tabrizi et al., 2009). It needs only simple set-up and has a potential for scaling-up to produce larger quantities by operating many parallel spark dischargers (Biskos et al., 2008). It is also useful for producing new mixed nanoparticulate materials which can be applied to advanced catalysis (Tabrizi et al., 2010).

The method was analyzed systematically by Tabrizi et al. They attempted the analysis about effective factors of particle formation such as breakdown voltage, gas pressure, gas flow rate, inner electrode gap, capacitance, spark repetition frequency, etc. (Tabrizi et al., 2009). The method is attracting widespread interest in fields such as increasing the efficiency of an organic light-emitting devices(OLEDs) by embedding nanoparticles into the active layer of that (Sung et al., 2014) and fabricating large-area three-dimensional nanoparticle-structure arrays (Ha et al., 2014).

Although the method has many benefits as mentioned above, there remain several challenges to be overcome. The first challenge is the agglomeration of spark-generated particles (park et al., 2014). Positive and negative ions produced by the spark-discharge interact with the nanoparticles in post spark region and then charge state of the nanoparticles converts to bipolar charge state on account of bipolar diffusion charging (Bau et al., 2010). Agglomeration tends to occur between bipolar nanoparticles. To prevent the post-discharge bipolar diffusion charging between nanoparticles, Tabrizi et al. (2009) controlled the parameters such as energy per spark, flow rate, spark repetition frequency, and carrier gas species. Han et al. (2012) utilized the pin-to-plate type spark generator. In the pin-to-plate type conFig.uration, agglomeration of particles could be lessened by fast transport of charged particles in the narrow exit hole of the plate electrode. Park et al. (2014) studied that the unipolar ion supplied by ionizer reduces the agglomeration of nanoparticles preventing post-discharge bipolar diffusion charging. However, previous researches have limitation with respect to controlling the agglomeration phenomenon by only the factors of pre spark discharge procedure as described above. The parameters of pre spark discharge procedure such as the components of circuit and gap distance cannot be changed during experiment and the change of parameter such as gas flow rate can have influence on another process of the experiment as well as size and amount of particles. Ha et al.(2014) showed the influence of flow rate on three dimensional nano-structure morphology in Fig. 2.1.

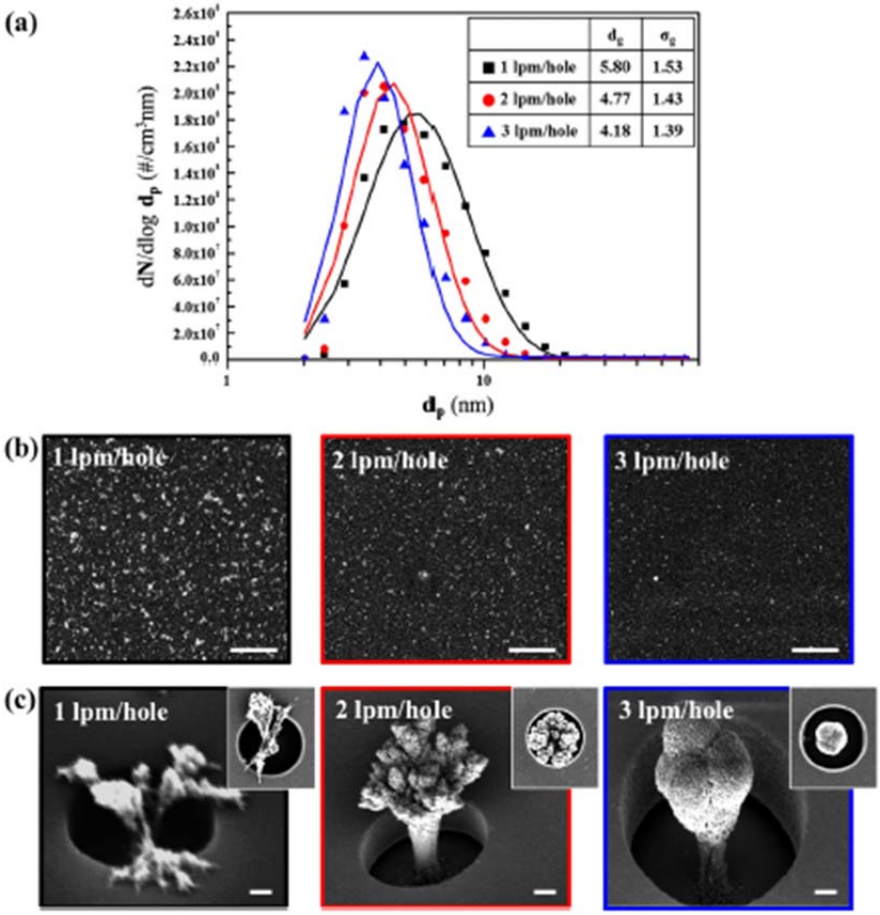

Figure 2.1. Size distributions measured by an SMPS system showing the decrease in the average diameter of the nanoparticles as the flow rate increases from 1, 2, to 3 lpm per hole.

(Adopted from Ha et al. 2014)

It needs to investigate the parameters of post spark regime which can affect the size and amount of nanoparticles without varying the initial condition of spark, namely the pre spark discharge procedure.

However few researches have been carried out on discovering the parameters of post spark discharge regime. It is required fundamental

research on the post spark discharge regime.

The second challenge is the generating a large amount of charged particles. Charged particles are utilized to construct multi-dimensional and multi-scale nanoparticle structures via ion assisted aerosol lithography (IAAL). Ion assisted aerosol lithography (IAAL) is the charged aerosol-based assembly technique, which uses the distorted local electric field induced by accumulated ions on a pre-patterned substrate. It is possible to control the trajectory of charged nanoparticles drawing to the substrate by electrostatic attraction (choi et al., 2015, kim et al., 2006, Lee et al., 2010, Ha et al 2014). A large amount of charged particles are needed to construct multi-dimensional nanoparticle structures in short time. However, few researchers have studied the increase of the amount of charged particles. Recently, Noh et al. (2016) developed spark dischargers for generating positively charged particles. But also the parameter of pre spark discharge procedure such as a modified spark discharge circuit was utilized in their research. There is a possibility that the generated ions might give a negative influence on the experiment. Therefore it is necessary to control the size and amount of charged nanoparticles by the new parameter in post spark discharge regime without varying other parameters in pre spark discharge procedure.

Motivated by these, in the present study, the new spark discharge generator was developed, which is capable of preventing agglomeration and generating a large amount of charged particles by utilizing the electric field effect in the post spark regime.

2.2. Experimental Concept

2.2.1. Spark discharge

Spark discharge is one of the most versatile techniques for generating nanoparticles in gas phase. This method is described in Schwyn et al. It has been applied by many research groups such as Evans et al., 2003 Evans et al. 2003 Horvath and Gangl 2003 Roth et al. 2004. The particles produced by this method are very similar to those obtained by laser ablation (Ullmann et al. 2002). This method can be applied to all conductive materials including semiconductors.

The spark discharge process is initiated by breakdown of the carrier gas and forms a conducting plasma channel. Rapid discharge is done with current associated with high temperature (typically 20000 K). As a result, the electrode material evaporates in the vicinity of the spark. Rapid cooling is initially dominated by adiabatic expansion and radiation. Cooling below evaporation temperature is governed by heat conduction. The spark generator is generally composed of an order chamber with a volume of several hundred cm 3 and two opposed cylindrical electrodes are set at adjustable distances.

The electrodes which are several millimeters in diameter and several millimeters apart are connected to a high voltage power supply and ground, and in parallel to a capacitor having a capacitance of some tens of nF.

The power supply supplies a constant current that periodically charges the capacitor after discharge occurs at breakdown voltage.

Electrical circuits including inductive components, which lead to damped

oscillating discharge processes with durations of a few microseconds.

During this oscillation, the current is temporarily reversed and the two electrodes are ablated. This is not the case with a unipolar discharge, because positive ions in the plasma collide the negative electrode more strongly than electrons collide the positive electrode. The spark frequency can generally be adjusted up to the order of kHz. If this frequency is exceeded, continuous discharge will occur. These high frequency process produces much larger particles (tens of nm in diameter), but rapid sparks bring nanoparticles with diameters less than 10 nm. The average particle diameter can be controlled by the energy per spark, which is determined by the capacitance and the distance between the electrodes. The mass of particles generated per unit time is proportional to the spark frequency.

If the flow rate of inert gas passing through the generator is sufficiently high with respect to the spark repetition frequency, unagglomerated particles a few nanometers in size can be obtained.

2.2.2. Comparison between Common Spark Discharge Generator (CSDG) and Post Spark Discharge Manipulator (PSDM)

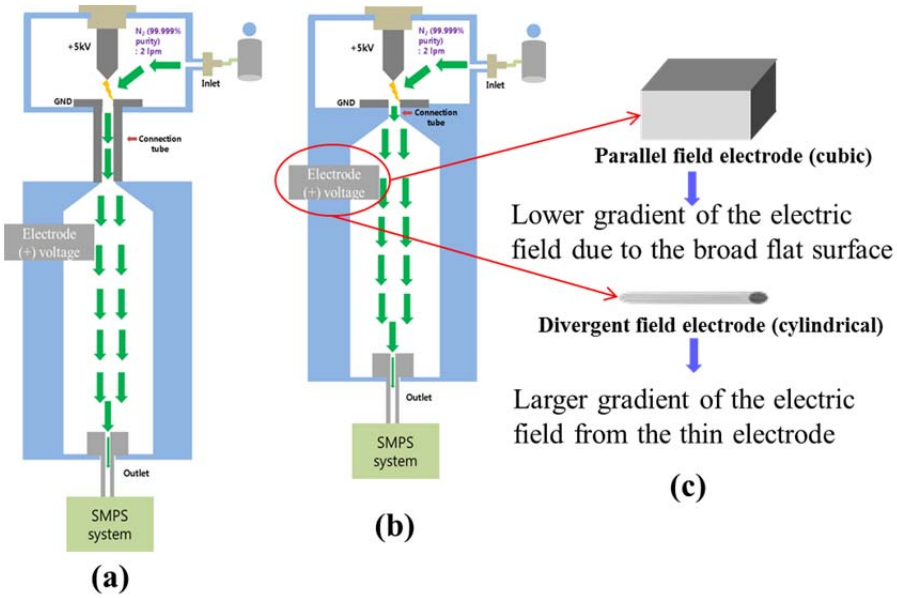

Figure 2.2. Schematics of spark discharge generators. (a) Common spark discharge generator (CSDG); (b) post spark discharge manipulator (PSDM); (c) Parallel, divergent field electrodes

Two different spark chambers depicted in Fig. 2.2: the common spark discharge generator (CSDG) and the post spark discharge manipulator (PSDM) exerted by electric field. Both generators consisted of two main parts: a spark discharge chamber and an electric field chamber.

These two chambers were designed to investigate the behavior of particles affected by electric field in post spark discharge regime. Though two spark

discharge generators were mostly the same, there was a difference: connection tube length. Tube length of the CSDG was 8.5mm and that of the PSDM was 1.5mm. The difference of the connection tube length means whether particles in the post spark dusty plasma are affected by electric field or not. Since the connection tube length of the CSDG was long, post spark dusty plasma generated by spark discharge has disappeared while dusty plasma cloud was passing through the tube. It is known that only particles undergoing aerosol formation and growth process are survived (Borra, 2006). Therefore, the survived particles could be affected by electric field upon passing through the tube of the CSDG. Whereas, in case of the PSDM, the connection tube length was much shorter than that of the CSDG. Hence, particles in dusty plasma are affected by electric field prior to disappearance of post spark dusty plasma.

Two spark-discharge chambers are equipped with two rod-like electrodes downstream so that either of them can be biased. In addition, the effect of the rod-like electrode shape (cubic electrode and cylindrical electrode) was investigated. The cubic electrode may give a lower gradient of the electric field due to the broad flat butt of the thick electrode compared to the larger gradient field from the cylindrical electrode because the flat part produces more homogeneous field thus reducing the gradient. Two types of electrodes were used: the cubic one of 2.4 cm width and the thin one of 3mm diameter to control the effect of electric field configuration. The cylindrical rod would create a more divergent electric field compared to the cubic rod.

The pin-shaped electrode was 99.99% copper and its diameter was 7 mm. It

was precisely placed at the center axis of the spark discharge chamber. The ground plate having the thickness of 2 mm was placed just beneath the pin electrode. There was a hole with a diameter of 1 mm in the center of the plate. Nitrogen gas (99.999% purity) was used as a carrier gas and it was set at the flow rate of 2 lpm. It flowed from the inlet of the spark discharge chamber to the outlet of the electric field chamber through the hole in the plate. The inlet of the electric field chamber was conical shape and its body was cylindrical shape. The height of the conical part was 14.5 mm, the height of the cylindrical shaped body part was 118 mm and the diameter of that was 36 mm. A cuboid copper electrode, that is, electric field generating electrode (EF electrode) was rigorously installed at 12 mm downstream from the top of the chamber. The electrode was tightly inserted into the interior of the chamber at a length of 10 mm.

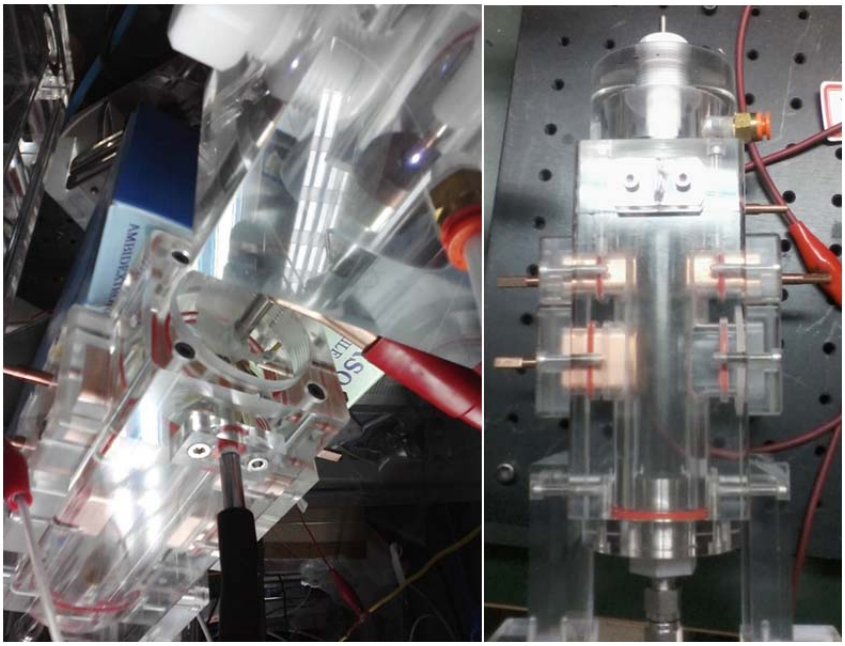

Figure 2.3. Picture of the spark discharge generator . (a) Common spark discharge generator (CSDG); (b) post spark discharge manipulator (PSDM).

These are real pictures. CSDG was described simply in the schematic of it in Fig. 2.3. In Fig. 2.3, CSDG consists of two chambers. Upper chamber is common spark chamber and it generated copper vapors due to the electrode melting by spark. They underwent nucleation and particle growth procedure then moved to lower chamber through the 8.5mm length tube and then they were affected by electric field. PSDM consists only one chamber and generated copper vapors also same as CSDG.

However, since tube length was shorter than one of CSDG, before undergoing nucleation and particle growth procedure, they were affected by electric field.

2.2.3. Electric circuit and experimental set-up for measuring the size distribution of nanoparticles

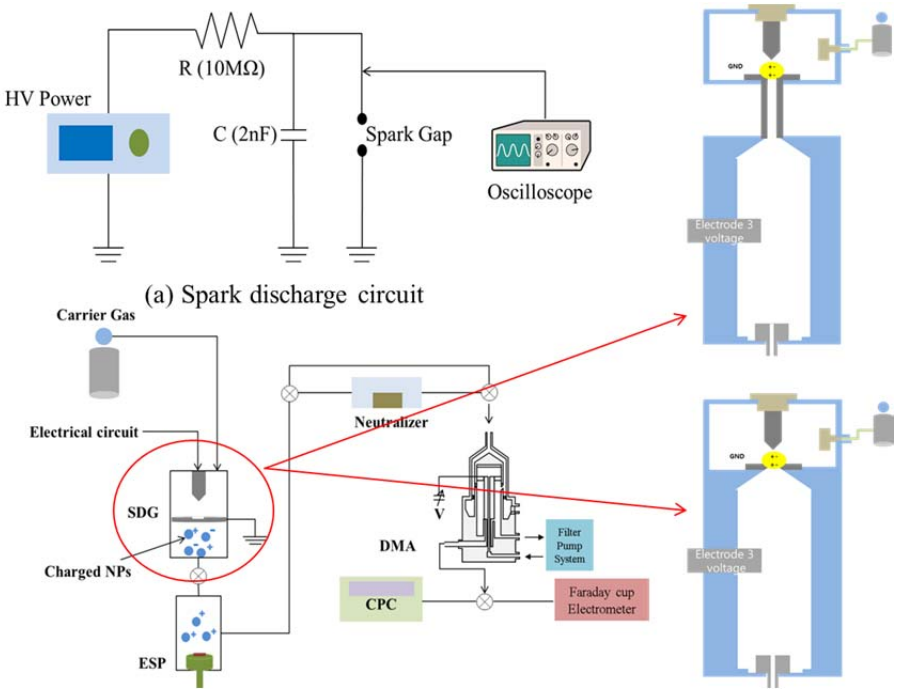

Figure 2.4. Experimental set-up for measuring the size distribution of the nanoparticles generated by CSDG and PSDM.

Fig. 2.4 shows a schematic diagram of the spark discharge circuit and experimental set-up. The circuit presented in Fig. 2.4 (a) was generally and widely used types of circuit (Han et al., 2012; Tabrizi et al., 2009). This circuit was composed of a 2nF capacitor and a 5MΩ resistor. 5kV potential was applied by the high voltage power supply (Fug HCP350 - 12500). Discharge voltage was measured by the high voltage probe (Tektronics

P6015A) connected to the oscilloscope (Agilent DSO-X 3014A). The measured discharge voltage (V_d) was about 3.75kV and the spark frequency was about 100Hz.

Figure 2.4 (b) shows the experimental set-up for measuring the size distribution of the nanoparticles generated by the CSDG and the PSDM. The CSDG and the PSDM were the SDG (spark discharge generator) part in Fig. 2.4 (b). The design of these two chambers was based on the design of the SDG fabricated by Han et al. (2012) and the aerosol transport part of the SDG was revised. Particles generated by spark discharge passed through neutralizer and thus their charge distribution was converted to Boltzmann charge distribution. Then, the particles were passed through a differential mobility analyzer (DMA). The particles were classified in size by the DMA. Then the number concentration of the selected particles was counted by a CPC. Total particle size distribution could be obtained through such a process. In the case of measuring the size distribution of positive particles, neutral and charged particles generated by spark discharge passed through the DMA without a neutralizer. Then, positive particles were classified in size with the voltage difference in the DMA and their number concentration could be counted by the CPC. The total particles consisted of neutral, positively charged, and negatively charged particles.

2.2.4. Influence of electric field on the initial condition of spark discharge

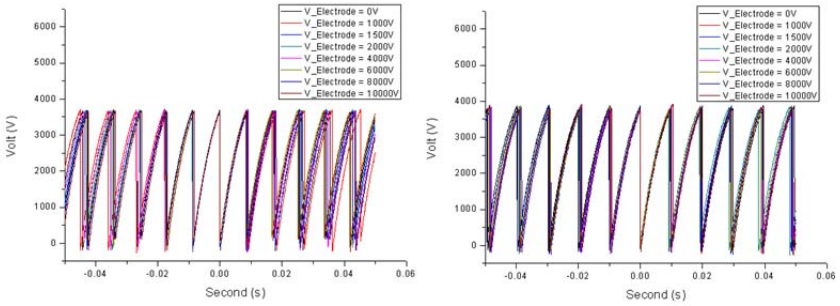

Figure 2.5. Discharge voltage profiles from (a) the common spark discharge generator and (b) the post spark discharge manipulator.

Figure 2.5 shows discharge voltage graphs according to the voltage of the EF electrodes of the CSDG and the PSDM. It was identified that voltage applied to the Electric Field (EF) electrode could not affect to the discharge voltage and the spark frequency. This phenomenon denotes certainly that initial condition (spark repetition frequency, energy per spark, gas flow rate, etc.) of spark discharge determining the particle size and amount is not affected by voltage of the EF electrode, which is able to avoid possibility that any initial condition factors are capable of affecting the results of the particle size distribution function.

2.3. Results and discussion

2.3.1. CSDG, PSDM particle size distribution in non-uniform E-field

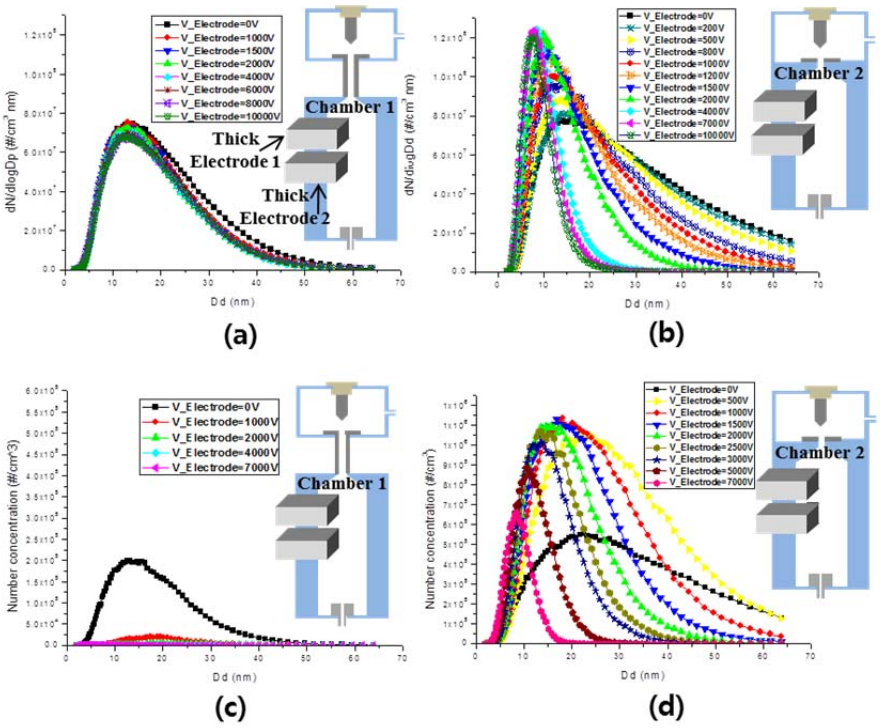

Figure 2.6. Total particle size distribution of (a) the CSDG and (b) the PSDM. The size distribution of positively charged particles of (c) the CSDG and (d) the PSDM. (freq=100Hz,V_d=3.75kV, N_2 flow rate = 2 lpm)

It was mentioned in the introduction that we developed the new spark discharge generator capable of preventing agglomeration and generating a

large amount of charged particles by utilizing the electric field effect in the post spark regime which is the internal factor of spark discharge process. Figure 2.6 illustrates total and positive particle size distribution of the CSDG and the PSDM according to the voltages applied to the EF electrode. Spark frequency, discharge voltage, and N_2 flow rate were 100Hz, 3.75kV, and 2 lpm, respectively. In order to investigate the electric field effect on the size distribution, voltage applied to the EF electrode was changed 0 to 10 kV.

Figure 2.6(a) and (b) display the total particle size distribution of the CSDG and the PSDM, respectively. Figure 2.6(a) and (b) shows the striking difference between the CSDG and the PSDM. As the voltage of the EF electrode increased, the total particle size distribution of the PSDM was drastically changed but that of the CSDG was changed a little. As shown in Fig. 2.6(b), the particle size was decreased and the number concentration of the small particles increased with the increase of the EF electrode voltage in the PSDM.

The dramatic difference between the CSDG and the PSDM was observed in the positive particle size distribution; evidence for this is in Fig. 2.6(c) and (d). The positively charged particles of the CSDG reduced extremely as can be found in Fig. 2.6(c). However, the positively charged particle size distribution of the PSDM showed a similar tendency as that of Fig. 2.6(b). It means that unagglomerated and positively charged particles were produced through the PSDM chamber. A general mechanism which could be understood from the analysis of the distributions in Fig. 2.6 (a) and (c) is

presented in the following. The charged particles move along the E-field lines and then the majority of them disappear by the loss attaching the electrodes (the plate and the EF electrode). Meanwhile, neutral particles having no charge are not affected by E-field. Since the proportion of the charged particles of the total amount of particles was very low as about 0.3%, total particle size distribution was rarely affected by the elimination of charged particles. In the case of Fig. 2.6(b) and (d), however, the results had a different tendency comparing to the common cases (Fig. 2.6(a), (c)). The size and amount of neutral particles changed surprisingly as well as that of charged particles changed by the electric field. It means that unagglomerated and a large amount of charged particle generation is affected by the electric field. Thus, in order to consider the effect of electric field, electric field simulation was inevitably carried out.

2.3.1. Electric field simulations of the CSDG and PSDM

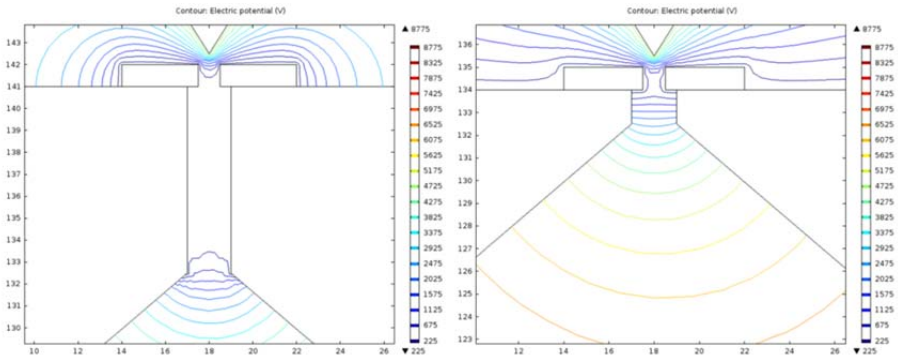

(a) (b)

Figure 2.7. Equi-potential lines resulted from electric field simulations of (a) the CSDG and (b) the PSDM. (Applied voltage of the EF electrode was 9kV).

Figure 2.7 shows the equi-potential lines resulted from the electric field simulations. In these two dischargers (CSDG and PSDM), nanoparticle generation regimes were the surface of pin and plate electrodes, but post spark regime affected by electric field was different. Post spark regime length of the CSDG was much longer than the PSDM. Thus, electric field simulations for the CSDG and the PSDM were carried out by the Comsol 4.3b simulation program to investigate the effect of the electric field in the post spark discharge regime. The voltage of the pin electrode was set 5kV, that of the plate electrode was set GND and that of EF electrode was set 9kV. As shown in Fig. 2.7(a), the connection tube region of the CSDG was not affected by the electric field since the voltage of that was zero. However, the connection tube region of the PSDM was affected by the electric field since the voltage of that was non-zero, as shown in Fig. 2.7(b).

In order to investigate the electric field effect in the connection tube region, the electric field strength was calculated along the length direction of that by line plotting through the center of the connection tube region.

2.3.2. Electric field strength along the connection tube

To explain why the PP-SDG generates much smaller and less-

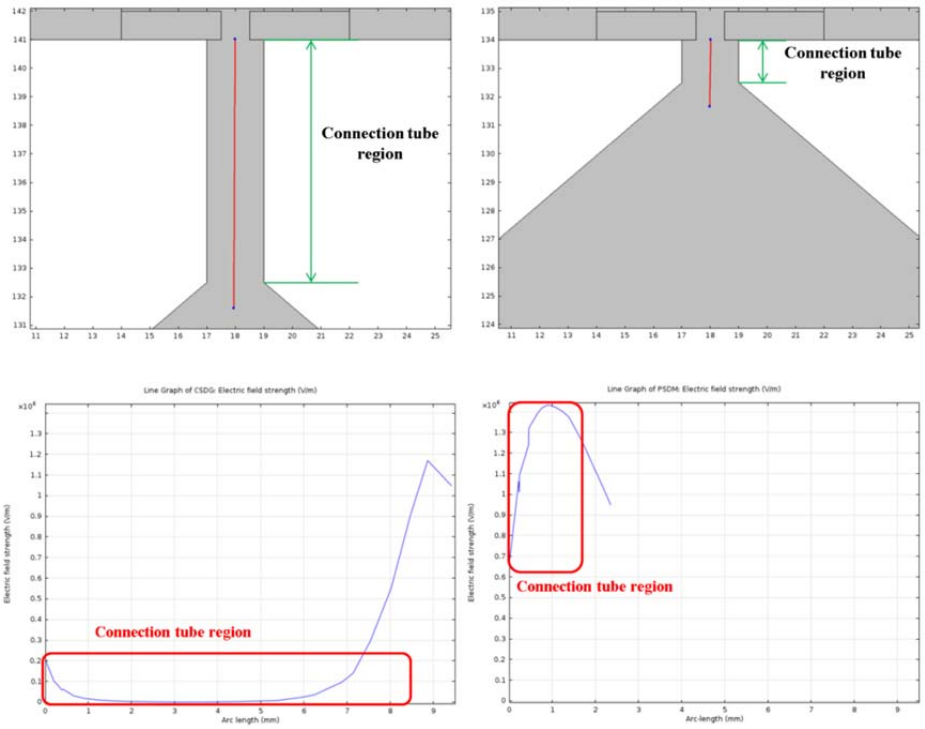

(a) CSDG (b) PSDM

Figure 2.8. The results of electric field strength along the connection tubes of (a) the CSDG and (b) the PSDM.

Figure 2.8 shows the electric field strength(V/m) in the connection tube region of the CSDG and the PSDM. In case of the CSDG, the value of electric field strength was almost zero in connection tube region (Arc length: 0 ~ 8.5 mm) where primary particles move from a spark discharge chamber to an electric field chamber. However, the value of electric field strength was

about $10^6(V/m)$ in connection tube region (Arc length: 0 ~ 1.5 mm) of the PSDM. It is apparent that particles generated immediately after spark discharge are affected by electric field in the PSDM.

2.3.5. E-field effect on the total number, volume concentration

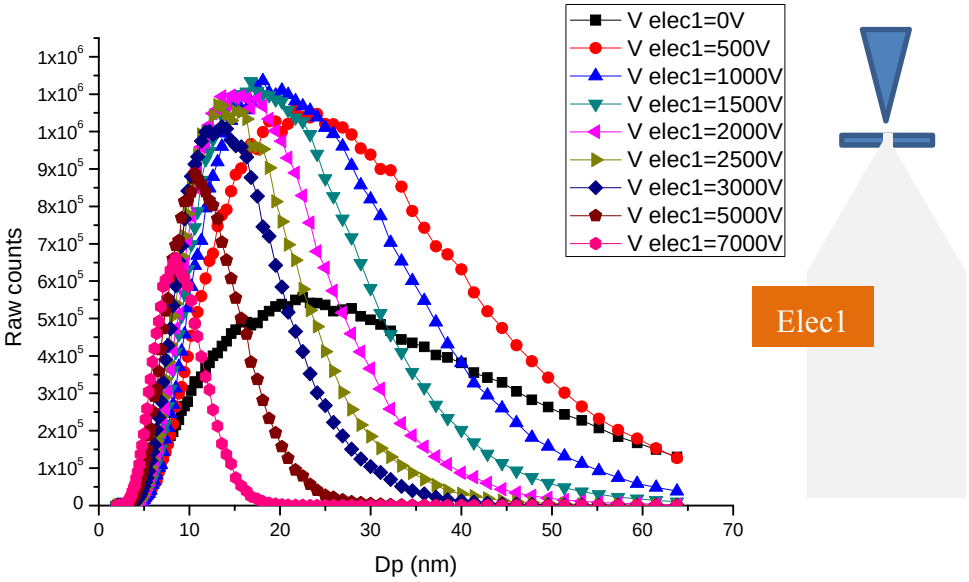

(a) Electric field effect on the particle size distribution

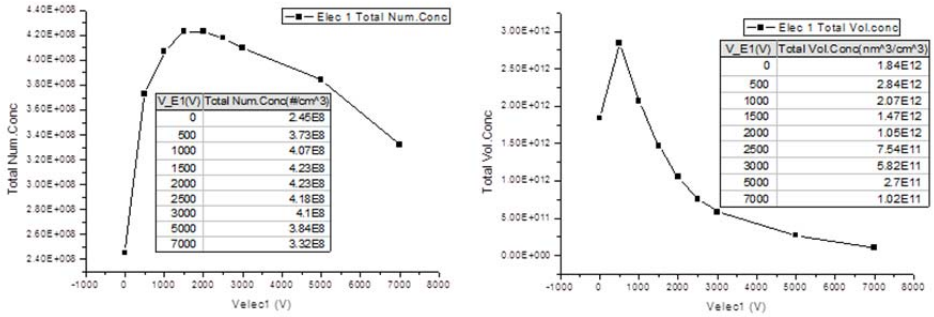

(b) E-field effect on the total number, volume concentration

Figure 2.9. E-field effect on the total amount of particles.

Figure 2.9 shows the electric field effect on the total particle number and volume concentration. Figure 2.9 (a) shows particle size distribution affected by voltage, that is electric field effect. Particle size distribution function moved towards to small sizes. As can be seen in Fig. 2.9 (b), total number and volume concentration was increased up to the critical voltage.

2.3.6. E-field effect on the high frequency condition

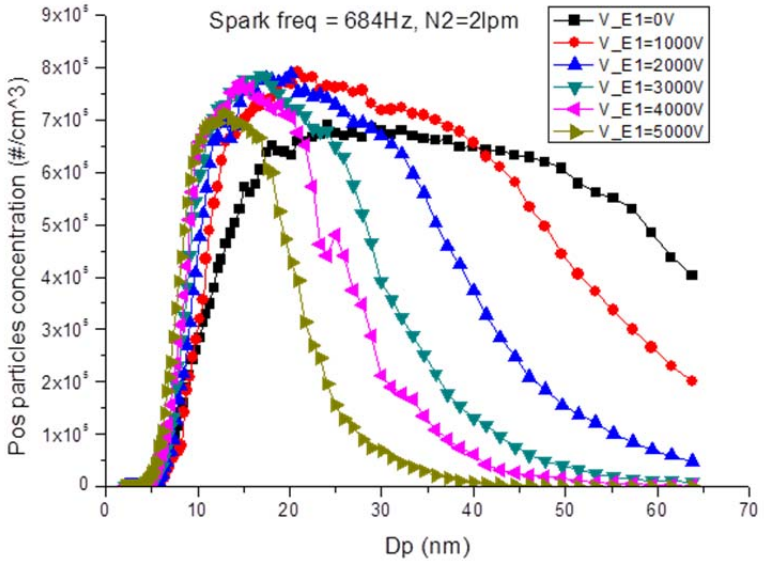

Figure 2.10. Positive particles size distribution at frequency 684Hz

As can be known by Fig. 2.10, electric field effect also affected on the high frequency spark condition. This result showed the effect could be applied to high frequency.

2.4. Conclusion

We developed the new spark discharge generator able to prevent agglomeration and generate a large amount of charged particles via controlling the post spark regime. As a result, it was found that the post spark discharge manipulator (PSDM) was an effective device to prevent agglomeration and generate a large amount of charged particles. Unagglomerated and positively charged particles were produced through the PSDM chamber due to the electric field effect. In addition, the size and amount of neutral particles changed surprisingly as well as that of charged particles changed by the electric field. Thus, it is apparent that electric field played an important role in the PSDM. After developing the PSDM, it could be applied to manufacture three dimensional nanostructures. As a result, well-patterned nanostructures were fabricated by using the PSDM. Therefore, it is expected that the PSDM could be utilized to prevent agglomeration fundamentally through controlling the post spark discharge regime.

2.5. References

Bau,S.,Witchger,O.,Gensdarmes,F.,Thomas,D.,&Borra,J.-P.(2010). Electrical properties of airborne nanoparticles produced by a commercial spark-discharge generator. Journal of Nanoparticle Research, 12, 1989–1995.

Biskos,G.,Vons,V.,Yurteri,C.,&Schmidt-Ott,A.(2008). Generation and sizing of particles for aerosol-based nanotechnology. KONA PowderParticle Journal, 26, 13–35.

Borra,J.-P.(2006). Nucleation and aerosol processing in atmospheric pressure electrical discharges: powders production, coatings and filtration. JOURNAL OF PHYSICS D: APPLIED PHYSICS 39, R19–R54.

Choi,H.,Kang,S.,Jung,W.,Jung,Y.,Park,S.,Kim,D.,&Choi,M.(2015). Controlled electrostatic focusing of charged aerosol nanoparticles via an electrified mask. Journal of Aerosol Science, 88, 90-97.

Evans,D.E.,Harrison,R.M.,&Ayres,J.G.(2003).The generation andcharacterisation of elemental carbon aerosols for human challenge studies. Journal of Aerosol Science, 34, 1023–1041.

Horvath,H.,&Gangl,M.(2003).A low-voltage spark generator for production of carbon particles. Journal of Aerosol Science, 34, 1581–1588.

Kim,H.,Kim,J.,Yang,H.,Suh,J.,Kim,T.,Han,B.,Kim,S.,Kim,D.,Pikhitsa,PV.,& Choi,M.(2006).Parallel patterning of nanoparticles via electrodynamic focusing of charged aerosols. Nature Nanotechnology, 1, 117–121.

Kim,W., Pikhitsa,PV., &Choi,M. Particle size selection in post-spark dusty plasma in non-uniform electric field. Applied Physics Letter Submitted 2016

Lee,H.,You,S.,Pikhitsa,PV.,Kim,J.,Kwon,S.,Woo,CG.,&Choi,M.(2011).Thre e-dimensional assembly of nanoparticles from charged aerosols. Nano Letters, 11, 119–124.

Noh,S.,Kim,D.,Park,S.,&Choi.M.Development of a spark discharger scheme for generating positively charged nanoparticles. Journal of Aerosol Science Submitted 2015

Roth C, Ferron GA, Karg E, Lentner B, Schumann G,Takenaka S, Heyder J (2004) Generation of ultrafine particles by spark discharging. J Aerosol Sci Technol 38, 228–235

Schwyn,S.,Garwin,E.,&Schmidt-Ott,A.(1988).Aerosol generation by spark discharge. Journal of Aerosol Science, 19, 639–642.

Sung,H.,Lee,J.,Han,K.,Lee,J.-K.,Sung,J.,Kim,D.,Choi,M.,Kim,C.(2014).

Controlled positioning of metal nanoparticles in an organic light-emitting device for enhanced quantum efficiency. Organic Electronics, 15(2),491-499.

Tabrizi,N.,Ullmann,M.,Vons,V.,Lafont,U.,&Schmidt-Ott,A.(2009a). Generation of nanoparticles by spark discharge. Journal of Nanoparticle Research, 11, 315–332.

Tabrizi,N.,Xu,Q.,vanderPers,N.,&Schmidt-Ott,A.(2010).Generation of mixed metallic nanoparticles from immiscible metals by spark discharge. Journal of Nanoparticle Research, 12, 247–259.

Park, K.-T., Farid, M. M., & Hwang, J. (2014). Anti-agglomeration of spark discharge-generated aerosols via unipolar air ions. Journal of Aerosol Science, 67, 144-156.

Ha, K., Choi, H., Jung, K., Han, K., Lee, J. K., Ahn, K., & Choi, M. (2014). Large-area assembly of three-dimensional nanoparticle structures via ion assisted aerosol lithography with a multi-pin spark discharge generator. Nanotechnology, 25(22), 225302. doi: 10.1088/0957-4484/25/22/225302

Han, K., Kim, W., Yu, J., Lee, J., Lee, H., Gyu Woo, C., & Choi, M. (2012). A study of pin-to-plate type spark discharge generator for producing unagglomerated nanoaerosols. Journal of Aerosol Science, 52, 80-88. doi: 10.1016/j.jaerosci.2012.05.002

Chapter 3.

Theoretical and experimental analysis of the post spark residual dusty plasma motion in non-uniform electric field

3.1. Introduction

The present study shown in chapter 2 verified that electric field parameter is able to change the size and amount of nanoparticles without varying any initial condition in spark discharge system. It is necessary to investigate the mechanism related to electric field effect precisely in order to utilize the effect to other applications. However few researchers have studied about the mechanism related to the post spark discharge regime, i.e., spark discharge mechanism due to the difficulty of measuring straightforward the region where the spark discharge takes place (Ludvigsson et al., 2015). Hence, indirect approach method is needed. It is expected that residual post spark complex (dusty) plasma maintains for short time after spark discharge. In lightning plasma, after lightning spark discharge takes place between sky and ground, residual post lightning spark plasma lasts about 10~100 milliseconds. When comparing with spark discharge, the residual post spark plasma lifetime can be estimated about 1 millisecond. Since the residual post spark complex plasma lasts about 1 millisecond, if the interaction between the post spark plasma and the forces acting on the plasma is analyzed, the mechanism can be verified. There are several forces acting on the dusts in complex (dusty) plasma such as ion drag force, electric force, weight force neutral drag, thermophoretic force (A.Piel 2010). Among these forces, electric force can be manipulated easily by changing electric field. It needs to consider the influence of electric force on the dusts in dusty plasma. In fact, electric field effects in complex (dusty) plasma have been a hot topic, especially when the

structures produced due to interactions of charged dust particles with plasma were found. The most spectacular structure is the redistribution of the particles in plasma resulting in a void generated inside the radio frequency (rf) plasma (Mikikian et al.,2010). The phenomenon manifesting the strong coupling of the dust particles to plasma is due to expelling particles out of central plasma regions to margins because of the ion drag while the electric field pushes the particles back thus forming the void with a well-defined boundary being in the dynamical equilibrium (Zafiu et al., 2003). One may expect that charged nanoparticles generated within spark discharge (that lasts less than one microsecond (Han et al., 2012)) and floating in the post-discharge plasma should also respond to non-uniform electric fields. However in spite of years of investigation none of such effects has been reported except for the case of patterning when the positively charged particles are guided by the configured electric fields long after residual post-spark plasma completely died at $t \gg \tau_p$ where τ_p is the post-spark plasma lifetime (Kim et al., 2006; Lee et al., 2011; Ha et al., 2014; Choi et al., 2015). Therefore, it was attempted to analyze the electric field effect to the particles in post spark dusty plasma in theoretically and experimentally in case of $t \lesssim \tau_p$, namely, the time before residual post spark plasma die.

3.2. Hypothesis about the post spark dusty plasma motion

3.2.1. Post spark dusty plasma in the process of nano-pattering

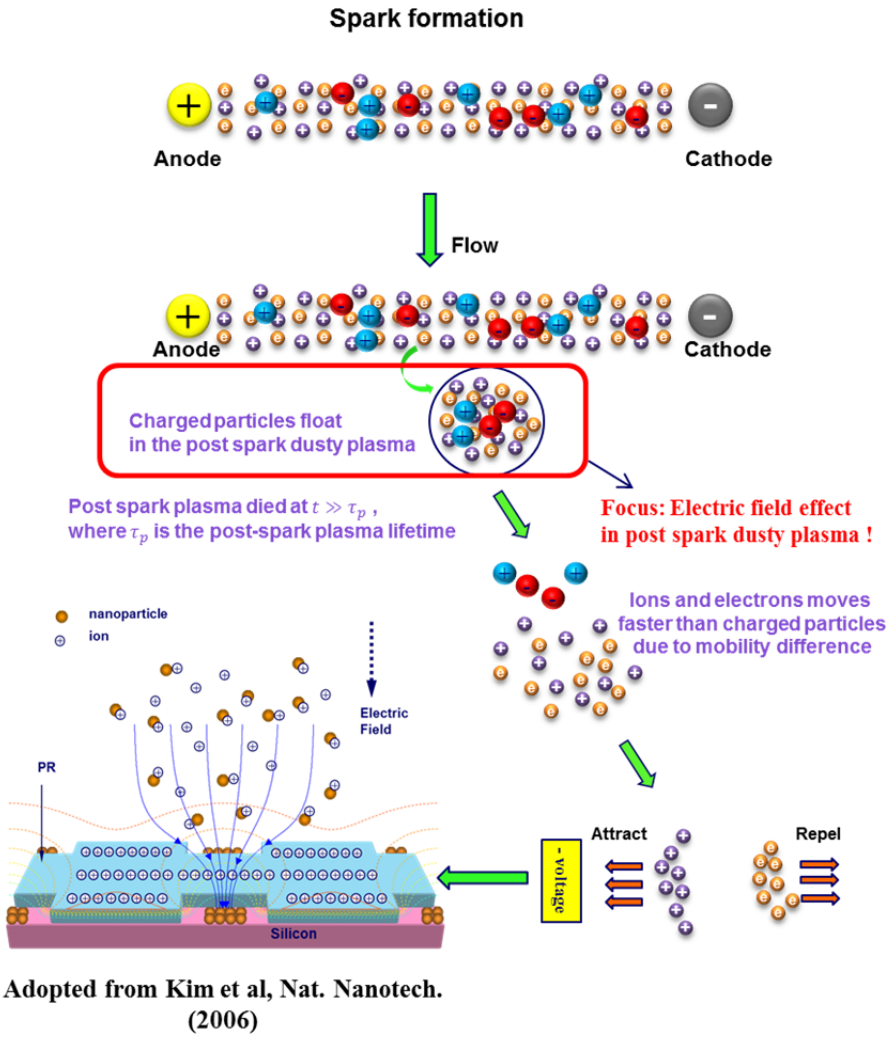

Figure 3.1. Post spark dusty plasma in the process of nano- pattering.

Figure 3.1 shows spark formation, transportation of charged nanoparticles and ion assisted aerosol lithography. Red color rectangular area describes charged particles floating in the post spark dusty plasma. This state is maintained very short time such as a few microseconds. After short time, post spark dusty plasma disappears and individual charged particles move along the electric field line. In previous research, there have been few research about the post spark regime. This concept is introduced first in this research.

3.2.2. Plasma lifetime

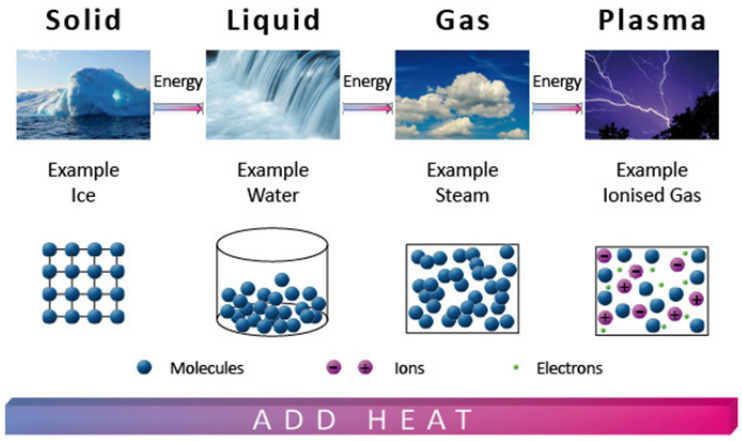

Figure 3.2. Several state of the matter including plasma state (Adopted from http://www.balticnet-plasmatec.org/plasma-technology/ 2016.10.26)

Plasma lifetime denotes the time maintaining post spark plasma condition. Plasma is high energy state and quasi-neutral state. So, in order to maintain the state, it needs high electrical energy, i.e., electric field. Generally, rf plasma is used widely to many areas. It is stationary plasma state, but spark

discharge is dynamic condition, so plasma state is maintained during very short time.

Figure 3.3. Lightning plasma

(Adopted from https://en.wikipedia.org/wiki/Lightning/ 2016.10.22)

Plasma is called the 4th state of the matter. Plasma consists of ions, electrons, neutral molecules, charged molecules having high energy state.

We can observe plasma easily in our environment. Lightning denotes a typical plasma phenomenon.

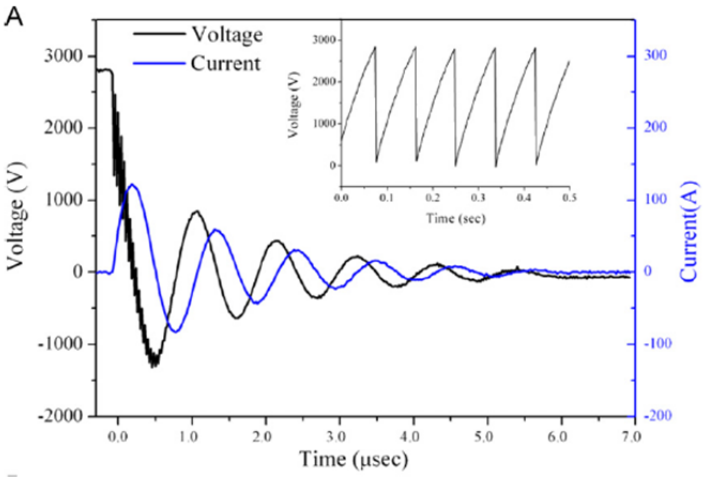

Figure 3.4. Voltage and current oscillation during spark discharge, inset shows the voltage oscillation with respect to time. (for positively and negatively charged particles of In–Sn alloy for each configuration with a gap distance of 2.5mm, argon gas flow rate of 3.5lpm and applied positive potential of 5 kV).

(Adopted from Han et al. 2012)

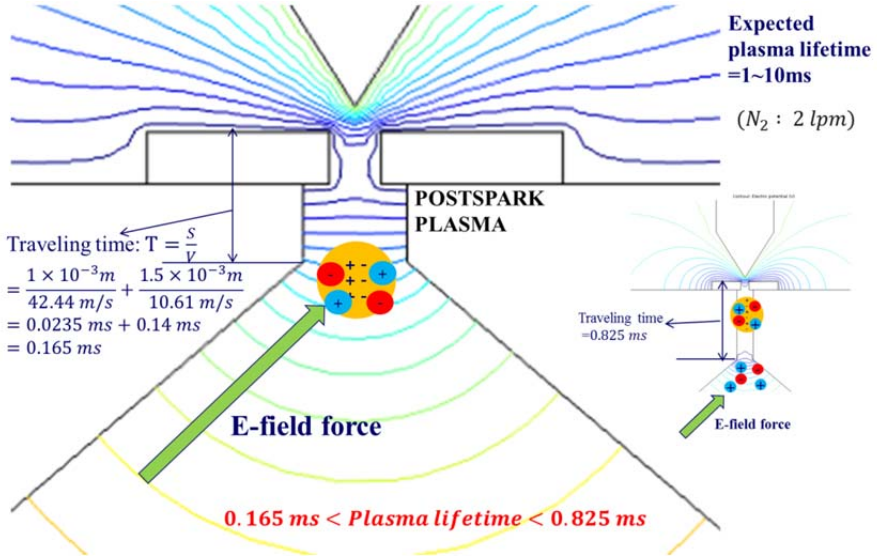

Figure 3.5. Post spark plasma lifetime

Particles generated immediately after spark discharge stay in plasma existed between the pin and the plate. Plasma containing particles is named dusty plasma. As lifetime of dusty plasma is very short, in case of the CSDG, dusty plasma has disappeared and only remained particles are affected by external electric field. However, in case of the PSDM, as electric field strength value is not zero in connection tube region, particles are affected by external electric field while staying in dusty plasma. In order to understand mechanism related to dusty plasma, it is needed to study the method of generating dusty plasma.

Capacitive radio frequency discharge commonly used to generate plasma is stationary condition and it maintains a continuous plasma state (C. Zafiu et al. 2003). Compared with that, however, spark discharge is dynamic condition combined with gas flow and plasma produced by spark disappeared in a short time of about $6 \times 10^{-6}s$ (Han et al. 2012) as can be seen in Fig. 3.4, yet the residual rarifying plasma (as our experiment shows) lasts milliseconds. As the dust particles are charged, the plasma can exhibit many new phenomena directly linked to the dust particles. Because the dust particles are massive compared to the other species of the plasma, the phenomena involving dust particle dynamics are relatively slow.

In case of the CSDG, particle traveling time moving through connection tube (where there is no electric field) is much longer than plasma lifetime, the particles are started being affected by the electric field only after post spark plasma has disappeared, therefore no effect of the electric field is observed.

However, in case of the PSDM, particles are affected by the electric field before residual plasma generated by the spark has disappeared. The clue for the phenomenon of the influence of the external electric field on the particle size distribution lies in the attraction of the plasma cloud to the electrode and in the difference in the coupling to plasma for large and small radius particles: as we will show elsewhere small particles are repelled from the dusty plasma cloud by the external electric field more effectively than large ones which results in the deformation of the particle size distribution function towards lower sizes as we observed. Additionally, small charged particles being separated from the plasma cloud repel one another more effectively thus preventing agglomeration and neutralization.

3.2.3. Forces acting on the particle in dusty plasma

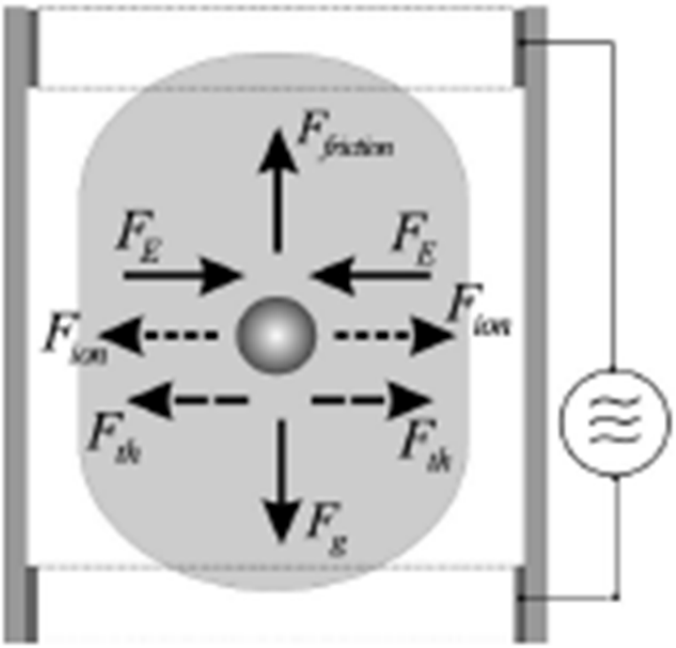

Figure 3.6. Forces acting on the dusts in stationary complex plasma (Adopted from C.Zafiu et al. 2003)

This figure shows forces acting on the dusts in stationary complex plasma. There are several forces such as gravity force, electric field force, ion drag force, thermophoretic force.

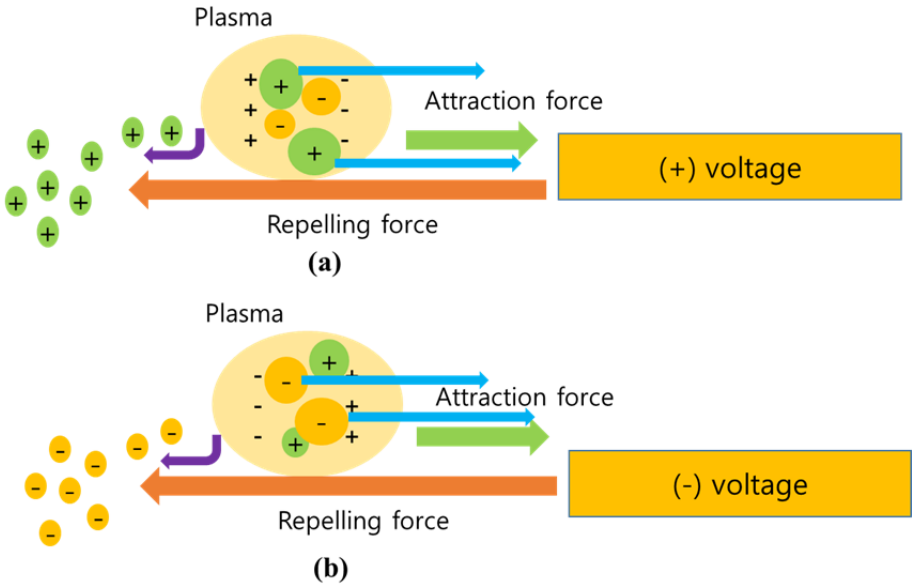

Figure 3.7. Forces acting on the particle in post spark dusty plasma at positive (a) and negative (b) electrode polarities.

In this work, as mentioned earlier, the analysis about forces acting on the post spark dusty (complex) plasma was carried out for finding the mechanism of the post spark regime. Figure 3.7 illustrates the forces acting on the particles in dusty plasma and the mechanism about the motion of post spark dusty plasma related to electric field. The large light-yellow circle denotes the plasma cloud including positive and negative particles, positive nitrogen ions and electrons. Large (large yellow and green circles) and small (small yellow and green circles) particles are dispersed in the plasma cloud and are affected by external electric field and ion drag forces. It is apparent that plasma cloud should not move in uniform electric field since its polarity is quasi-neutrality. However, the motion of plasma cloud represents striking difference in non-uniform electric field. As can be known from the

equipotential lines of the PSDM in Fig. 3.5, electric field generated by the EF electrode was non-uniform electric field. When post spark residual dusty plasma is affected by non-uniform electric field, plasma cloud having quasi-neutral property is polarized because of the gradient of electric field. Consequently, regardless of whether the polarity of EF electrode voltage is positive or negative, plasma cloud is attracted to the electrode (see Figure 3.7). In general, several forces act on the particles in dusty plasma such as weight force, electric force, ion drag force, thermophoresis force, etc. Electric force is originated from electric field generated by ions in plasma sheath area, ion drag force is generated by ion winds in plasma and thermophoresis force is generated by gradient of gas temperature (A. Piel, 2010). Although gravity force and thermophoresis force play an important role in general dusty plasma experiments, in our work, their contribution is negligible due to the fact that nano-size particle was used and the experimental temperature condition was constant. Therefore, ion drag and electric forces act on the particles dominantly (A. Piel, 2010).

3.3. Post spark plasma motion by several forces

3.3.1. Q_d in rf plasma and post spark plasma

Dp (μm)	Average No. Of Charges	Percentage of particles carrying the indicated number of charges								
		< -3	-3	-2	-1	0	+1	+2	+3	>+3
0.01	0.007				0.3	99.3	0.3			
0.02	0.104				5.2	89.6	5.2			
0.05	0.411			0.6	19.3	60.2	19.3	0.6		
0.1	0.672		0.3	4.4	24.1	42.6	24.1	4.4	0.3	
0.2	1.00	0.3	2.3	9.6	22.6	30.1	22.6	9.6	2.3	0.3
0.5	1.64	4.6	6.8	12.1	17.0	19.0	17.0	12.1	6.8	4.6
1.0	2.34	11.8	8.1	10.7	12.7	13.5	12.7	10.7	8.1	11.8
2.0	3.33	20.1	7.4	8.5	9.3	9.5	9.3	8.5	7.4	20.1
5.0	5.28	29.8	5.4	5.8	6.0	6.0	6.0	5.8	5.4	29.8
10.0	7.47	35.4	4.0	4.2	4.2	4.3	4.2	4.2	4.0	35.4

Table 3.1. Aerosol charge cistribution at Boltzmann equilibrium (Adopted from Hinds 1999)

The crucial difference between particles in rf plasma and in the post-spark plasma is that the charge Q_d on nanoparticles in rf plasma is proportional to the particle radius r_d (Barnes et al. 1992):

$$Q_d = \varphi_f r_d \qquad \textbf{[Equation 3.1]}$$

where φ_f is the floating potential while the charge on all charged particles in the post-spark plasma remains unitary $Q_d \sim 1e$ as our experiments demonstrate (Wiedensohler et al. 1988; Yoon. 2015).

In case of micron particles, ion drag force is proportional to the square of

particle radius and electric force is proportional to particle radius. These two forces are coupled and then act on the particles in plasma (A. Piel. 2010). However, in our research, since less than seventy nanometer size particles are treated, the effect of two forces was different. The charge equation of particle in dusty plasma, $Q_d = (\varphi_p - \varphi_s)4\pi\epsilon_o r_d(1 + \frac{r_d}{L})$ (Barnes et al. 1992), can be simplified as

$$Q_d = \varphi_f r_d \qquad \textbf{[Equation 3.2]}$$

Here verification experiments was carried out.

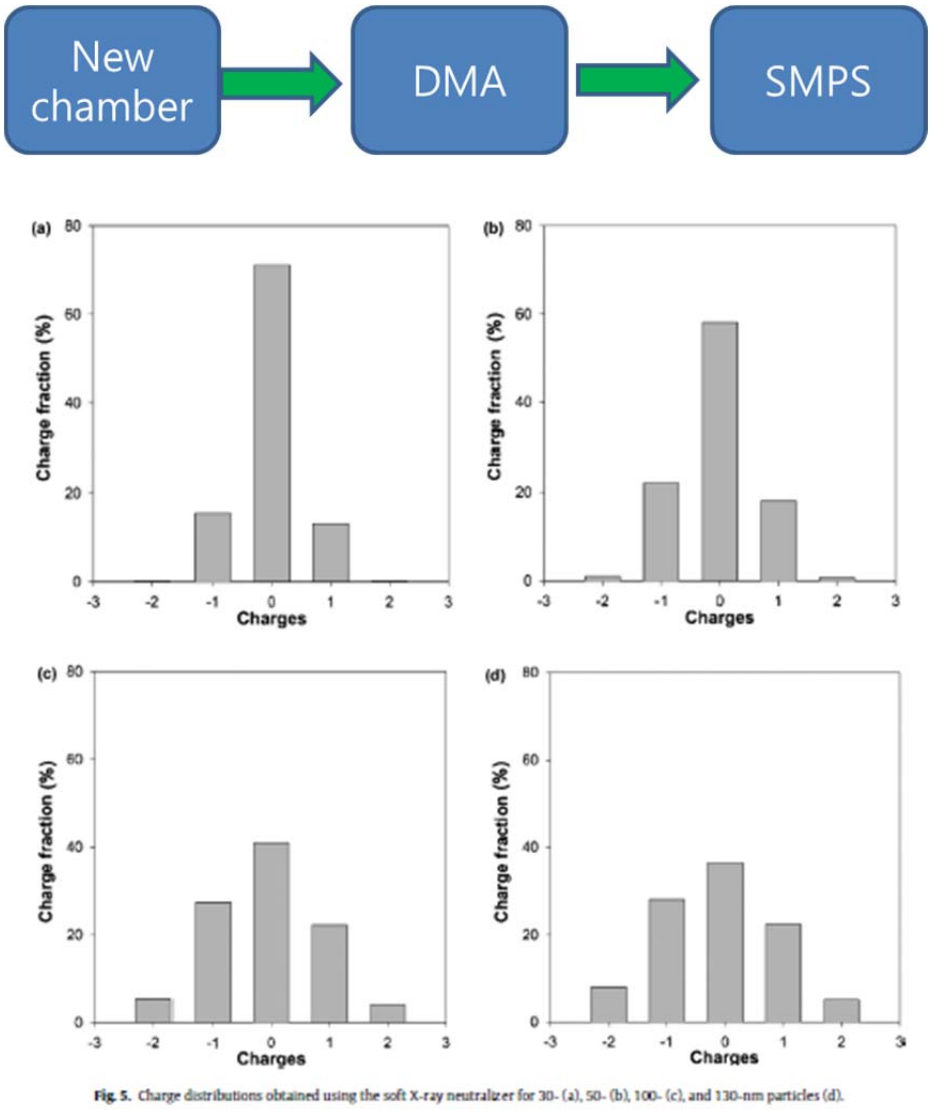

Fig. 5. Charge distributions obtained using the soft X-ray neutralizer for 30- (a), 50- (b), 100- (c), and 130-nm particles (d).

Fig. 3.8. Tandem DMA experiment procedure flow and Charge distribution obtained using the soft X-ray neutralizer for (a) 30_, (b) 50_, (c) 100_, (d) 130_ nm particles.

(Adopted from Y.H Yoon et al. 2015)

As can be known from above Fig. 3.8, in case of the size smaller than 50nm, most of all particles are neutral and unitary charged particles. Almost no highly charged particles exist.

Actually, experiments were carried out to demonstrate the charge fraction.

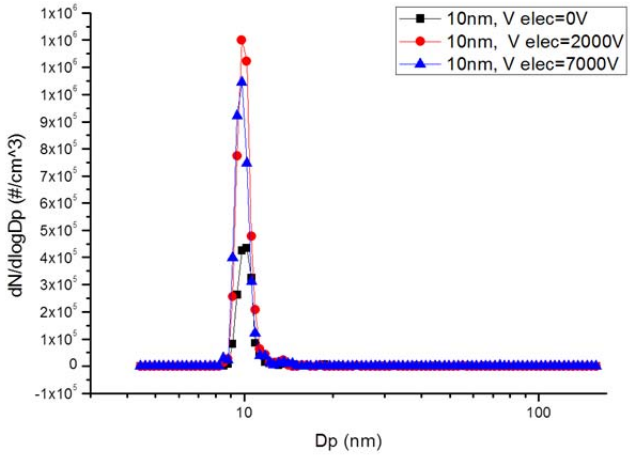

Figure 3.9. Tandem DMA experiment for 10nm particles

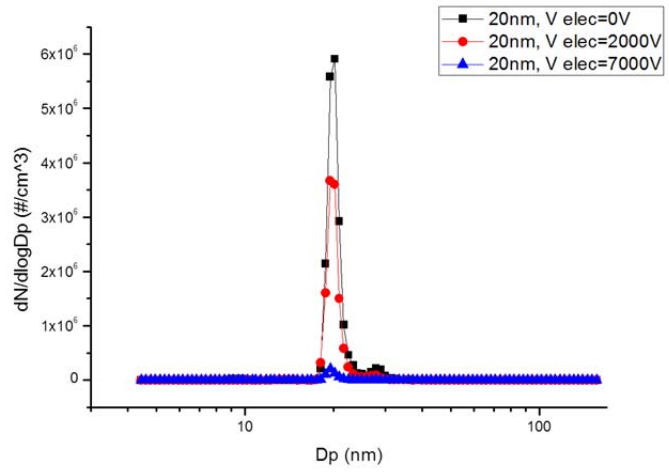

Figure 3.10. Tandem DMA experiment for 20nm particles

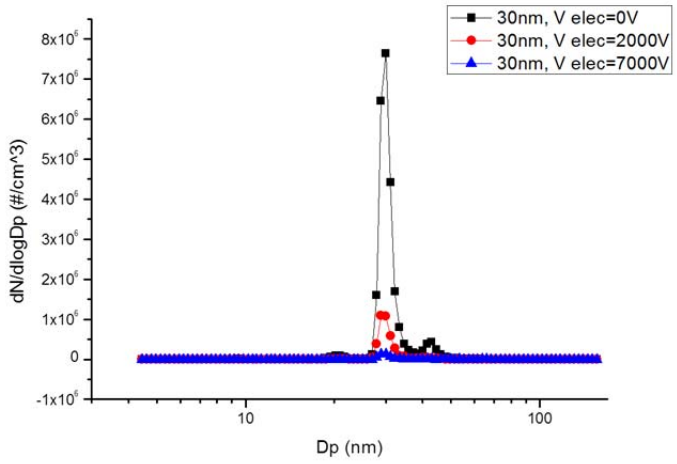

Figure 3.11. Tandem DMA experiment for 30nm particles

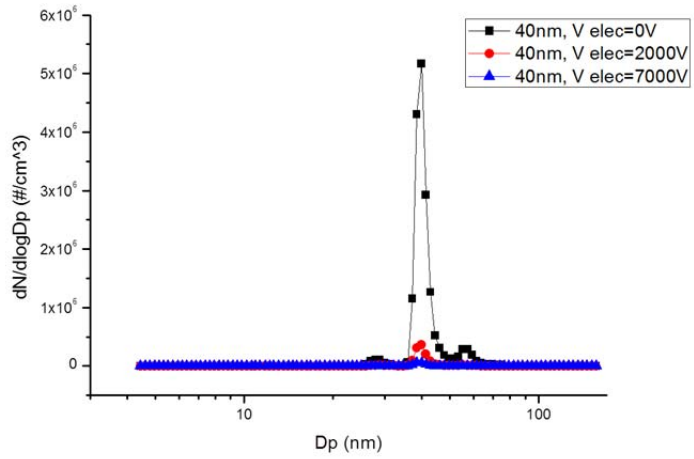

Figure 3.12. Tandem DMA experiment for 40nm particles

Through tandem DMA experiment, it was demonstrated that no highly charged particles are existed.

3.3.2. Electric force and ion drag force in post spark plasma

Name	Origin	Size dependence
Weight force	gravity	a^3
Neutral drag	streaming neutrals	a^2
Ion drag force	streaming ions	a^2
Thermophoresis	temperature gradient	a^2
Electric force	electric field	a^1

Table 3.2. External forces on dust particles (Adopted from A. Piel et al. 2010)

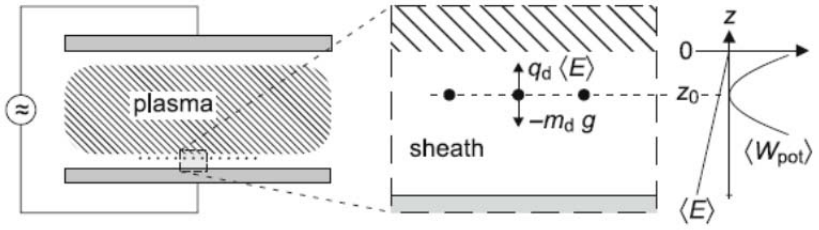

Fig. 10.14 Dust particles > 2 μm diameter sediment to the lower sheath of a radio-frequency operated parallel plate discharge, where the electric field force becomes sufficiently strong to balance the weight of the particle and levitate the particles in a thin layer

Figure 3.13. Interaction between the electric force and the weight force in plasma (Adopted from A.Piel et al. 2010)

The table informs the relationship between forces and size dependence. Fig 3.13 shows the equilibrium between gravity force and electric field force.

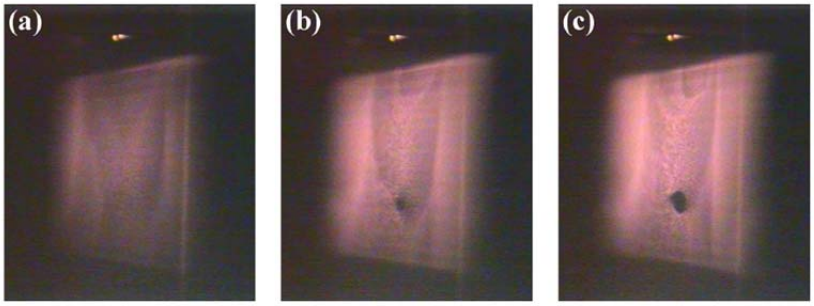

Fig. 1 Appearence of a void in the center of a dust cloud. Dust particles are growing from (a) to (c), the size in (c) is about a few hundreds nm. The view angle is about 20° with respect to the laser direction.

Figure 3.14. Appearance of a void in the center of a dust cloud due to ion drag force. (Adopted from Mimikan et al. 2010)

$$\mathrm{F_e} = \mathrm{Q_d E} \qquad \textbf{[Equation 3.3]}$$

As can be known from the charge equation, particle charge is proportional to the radius of particle, but in our research, electric force is proportional to electric field such as $F_e = (Q_d \sim 1)E$, since less than seventy nanometer size particles having unitary charge are used. Therefore, electric force affects all generated particles regardless of the radius of particles, ion drag force affects comparatively larger particles. On account of this reason, smaller particles, that is, particles whose size is below the some critical size as the border are expelled outside of the plasma cloud by external electric field.

The consequence of this is that the ratio of the electric force (directed from the positively charged rod)

$$\overrightarrow{F_e} = Q_d \vec{E} \qquad \textbf{[Equation 3.4]}$$

to the ion drag force[6] that acts in the direction of the motion of the plasma cloud

$$\overrightarrow{F_i} = n_i v_s m_i \overrightarrow{v_i} \pi {r_d}^2 \qquad \textbf{[Equation 3.5]}$$

(where n_i is ion concentration, $v_s = \sqrt{\frac{8T_i}{\pi m_i} + \overrightarrow{v_i}^2}$, T_i is the ion temperature, m_i is the mass of ions, and $\overrightarrow{v_i}$ is the ion velocity) is proportional to $1/{r_d}^2$ for the post-spark plasma instead of $1/r_d$ in the case of rf plasma. This means that the action of the external field is greatly enhanced for small size particles in case of post-spark plasma. While larger radius charged particles are dragged by the plasma cloud which moves in the non-uniform field as a whole towards the electrode and out of the gas stream, the charged particles which size is less than a certain size are pushed away from the cloud and remain in the gas stream charged and thus unagglomerated. As we show below this simple mechanism explains the whole set of experiments on the evolution of the PDF with the voltage towards smaller particle sizes.

3.4. Post spark plasma cloud motion in non-uniform E-field

3.4.1. Polarized spherical plasma cloud

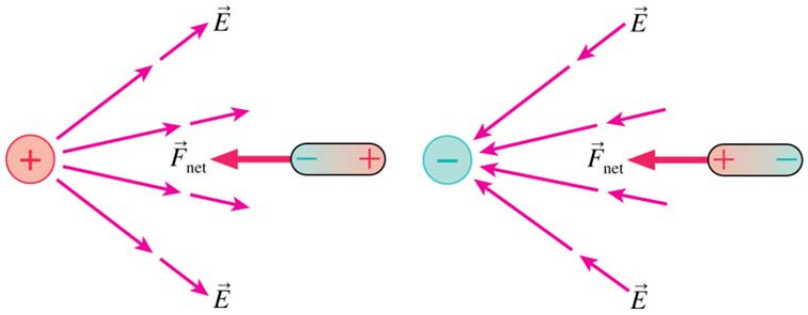

Figure 3.15. Dipoles in a Non-uniform Electric Field about $|\nabla(dE)|$ (Adopted from "Electric potential energy of point charges and dipoles.ppt")

Plasma cloud is a quasi-neutral state. But in non-uniform electric field, plasma cloud is polarized and then it moves by electric field. Regardless of the sign, plasma cloud moves by electric field.

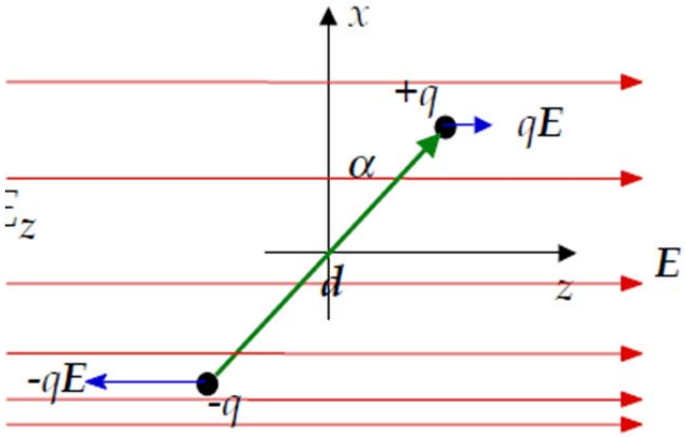

Figure 3.16. Force in a Non-uniform Electric Field

(Adopted from "Dipole in non-uniform Electric field.pdf")

Figure 3.16 shows the forces in a non-uniform electric field. Due to this asymmetric electric field, net force is generated.

Figure 3.17. Equipotential lines simulated by comsol 4.3b

This figure shows equipotential lines simulated by consol.

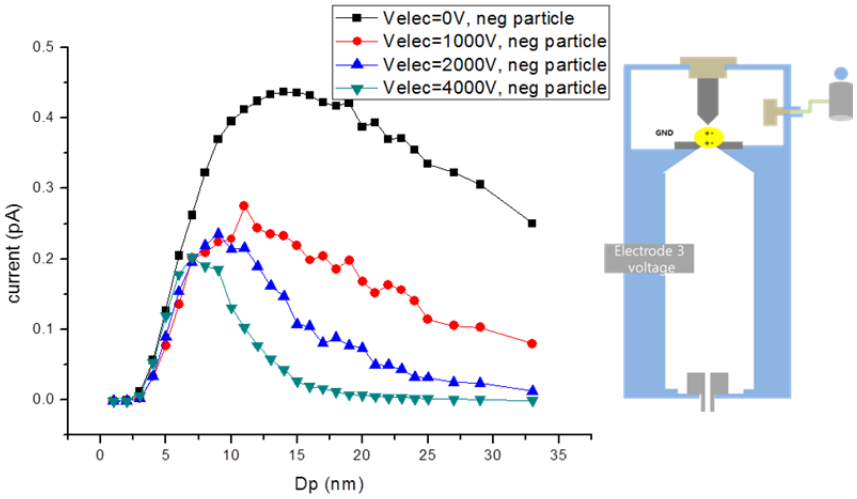

Figure 3.18. Negative particle size distribution in positive polarity E-field measured by electrometer (lower port suction, electrode 2)

Figure 3.18 shows negative particle size distribution in positive polarity E-field measured by electrometer (lower port suction, electrode 2). This is opposite result to the positive particle size distribution.

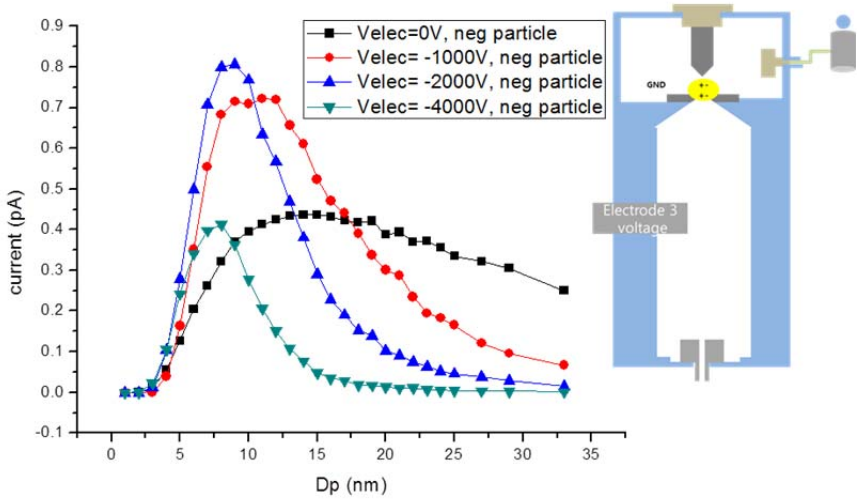

Figure 3.19. Negative particle size distribution in negative polarity E-field measured by electrometer (lower port suction, electrode 2)

Figure 3.19 shows negative particle size distribution in negative polarity E-field measured by electrometer (lower port suction, electrode 2)

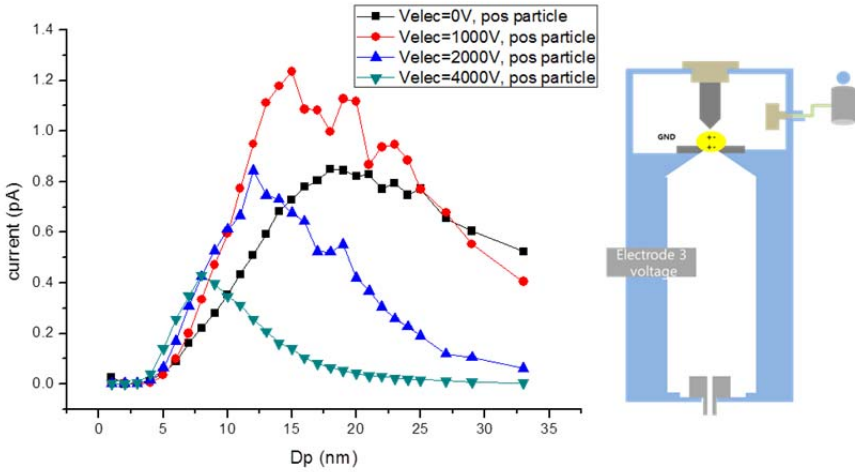

Figure 3.20. Positive particle size distribution in positive polarity E-field measured by electrometer (lower port suction, electrode 2)

Figure 3.20 shows positive particle size distribution in positive polarity E-field measured by electrometer (lower port suction, electrode 2). This result is similar with the result of the Fig 3.19.

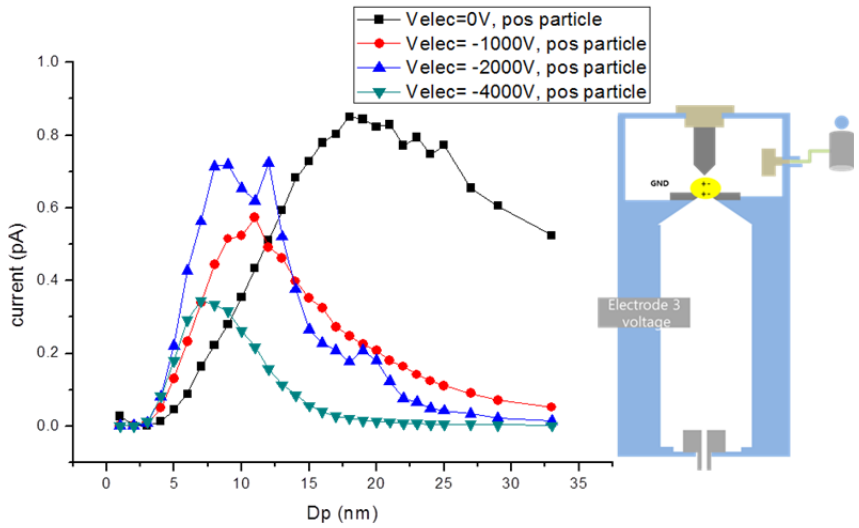

Figure 3.21. Positive particle size distribution in Negative polarity E-field measured by electrometer (lower port suction, electrode 2)

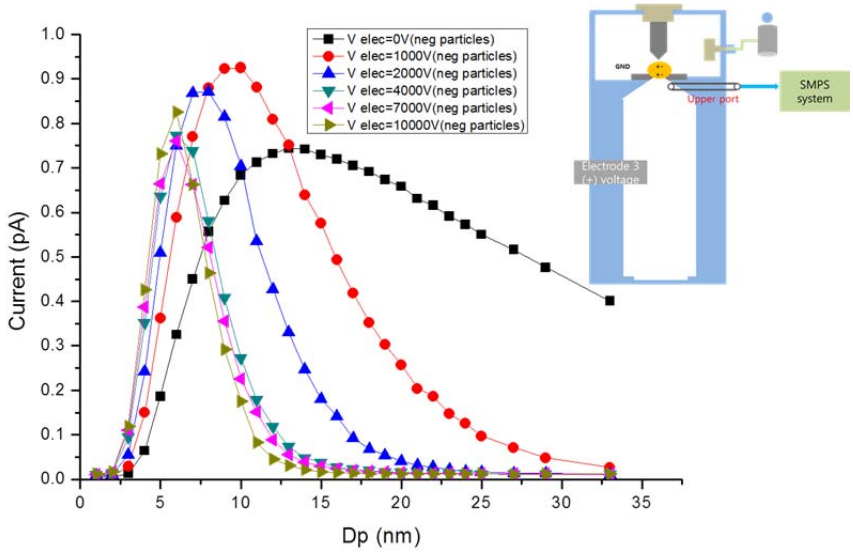

Figure 3.22. Negative particle size distribution in Positive polarity E-field measured by electrometer (lower port suction, electrode 2)

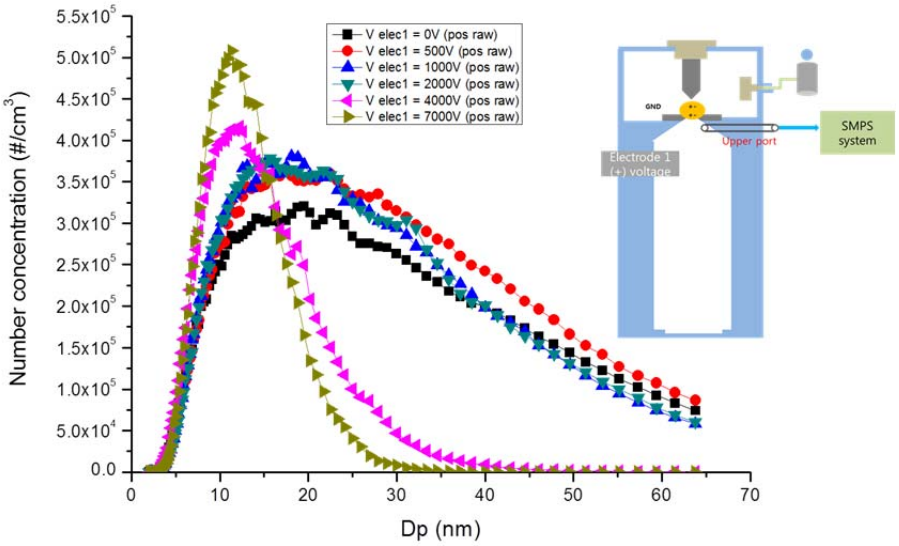

Figure 3.23. Positive particle size distribution in Positive polarity E-field measured by SMPS (lower port suction, electrode 2)

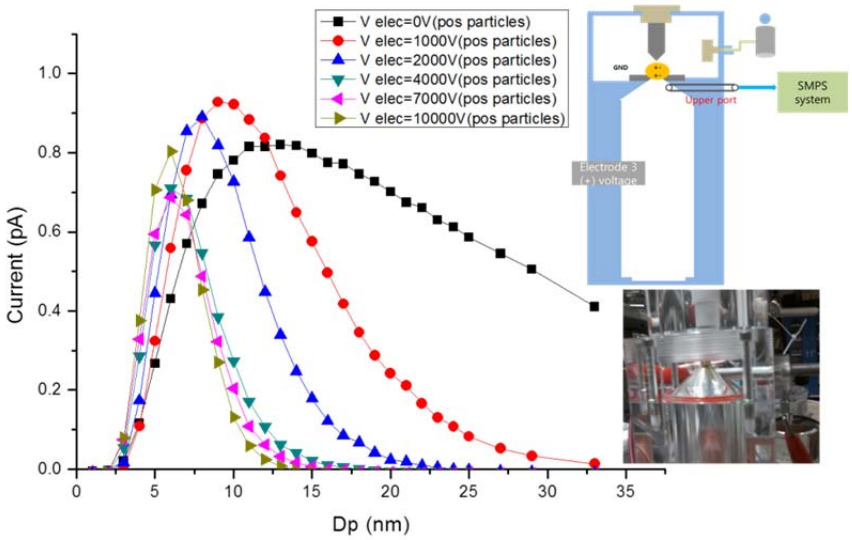

Figure 3.24. Positive particle size distribution in Positive polarity E-field measured by electrometer (<u>Upper port suction</u>, electrode 2)

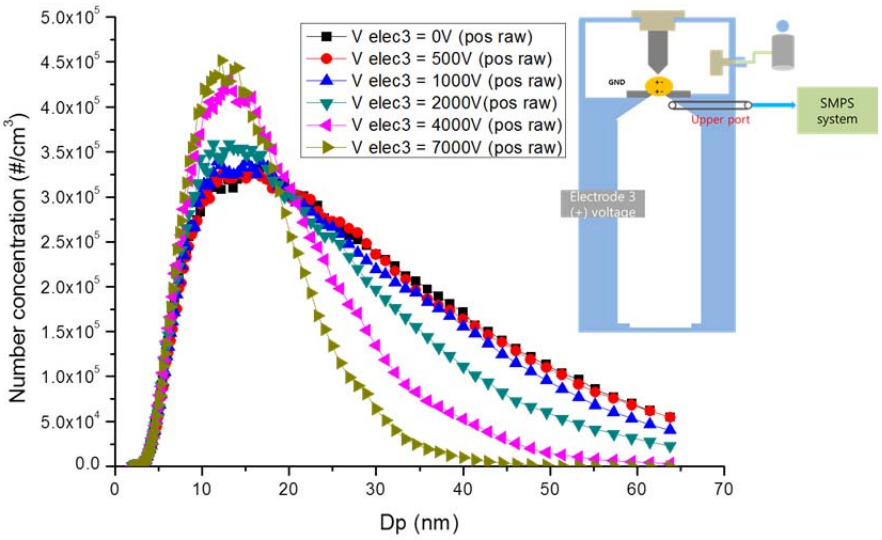

Figure 3.25. Positive particle size distribution in Positive polarity E-field measured by SMPS (Upper port suction, electrode 2)

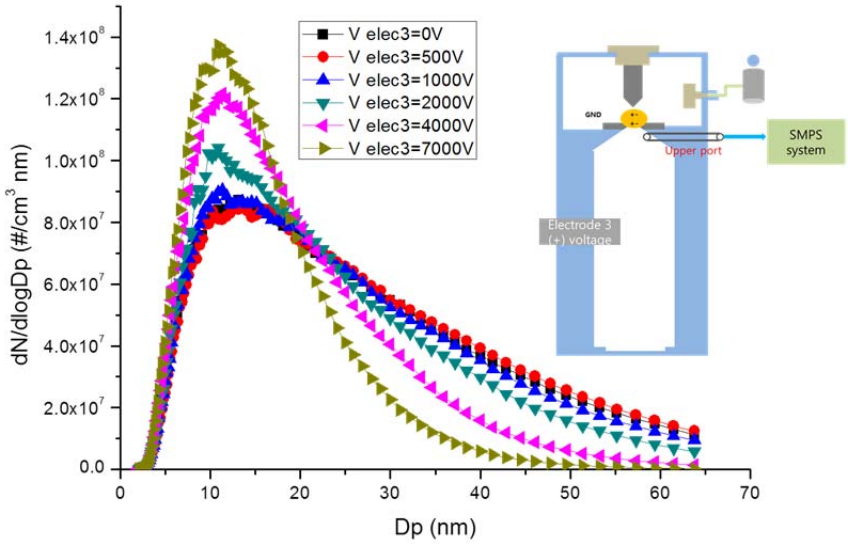

Figure 3.26. Total particle size distribution in Positive polarity E-field

measured by SMPS (Upper port suction, electrode 2).

3.4.2. Effect of E-field gradient on the particle size distribution

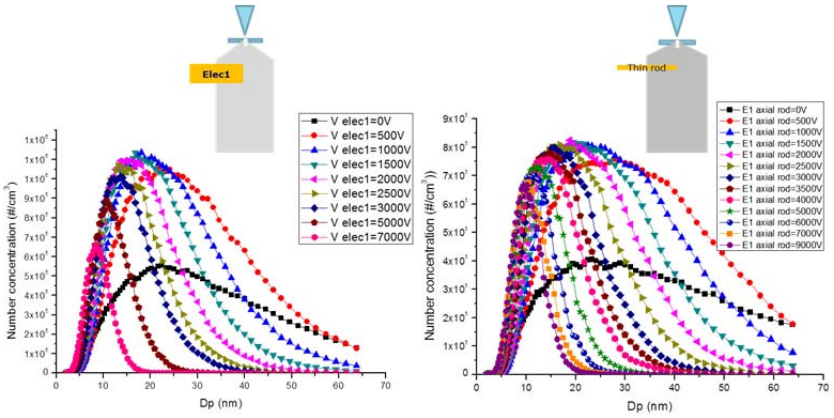

(a) (b)

Figure 3.27. Effect of E-field gradient on the particle size distribution for thick and thin electrode.

The experimental set-up was described in a recent work of our group in detail. Briefly, the part of schematic is shown in the insets in Fig. 2.2. where two spark-discharge chambers are equipped with two rod-like electrodes downstream so that either of them can be biased. In addition, the effect of rod-like electrode shape (thick and thin) was investigated. The thick electrode may give lower gradient of the electric field due to the broad flat butt of the thick electrode compared to the larger gradient field from the thin electrode because the flat part produces more homogeneous field thus

reducing the gradient. We used two types of electrodes: the thick one of 2.4 cm width and the thin one of 3 mm diameter to control the effect of electric field configuration. The thin rod would create a more divergent electric field being in position 1 (Fig.3.27.(b)) compared to the thick rod being in position 1 (Fig.3.27.(a)) close to other electrodes, yet fields for thin and thick electrodes would be similar at lower downstream position 2 .

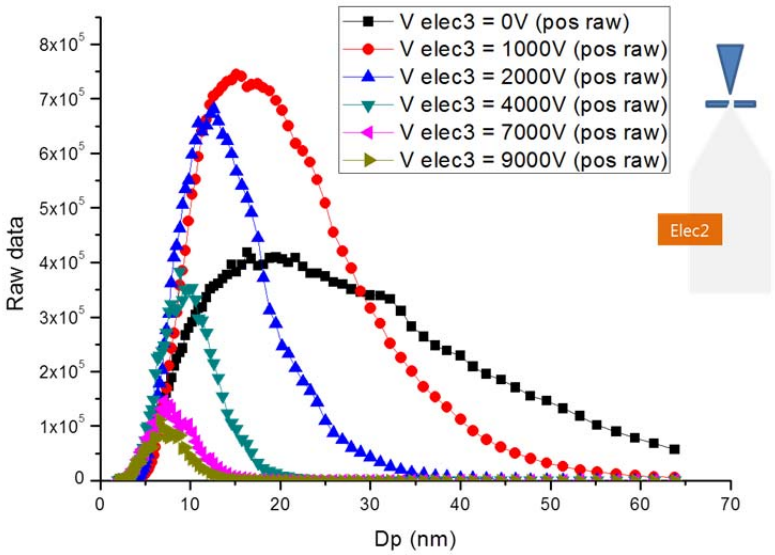

Figure 3.28. Positive particle size distribution in Positive polarity E-field measured by SMPS (Lower port suction, electrode 2).

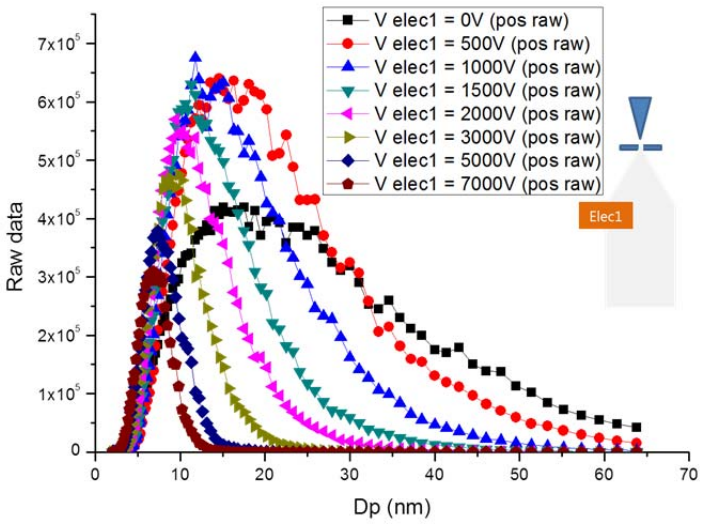

Figure 3.29. Positive particle size distribution in Positive polarity E-field measured by SMPS (Lower port suction, electrode 1).

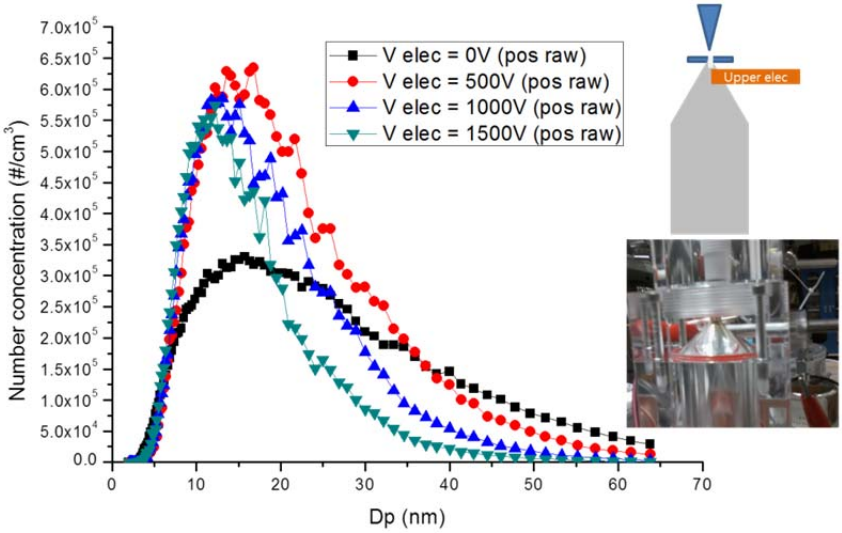

Figure 3.30. Positive particle size distribution in Positive polarity E-field measured by SMPS (Lower port suction, Upper electrode).

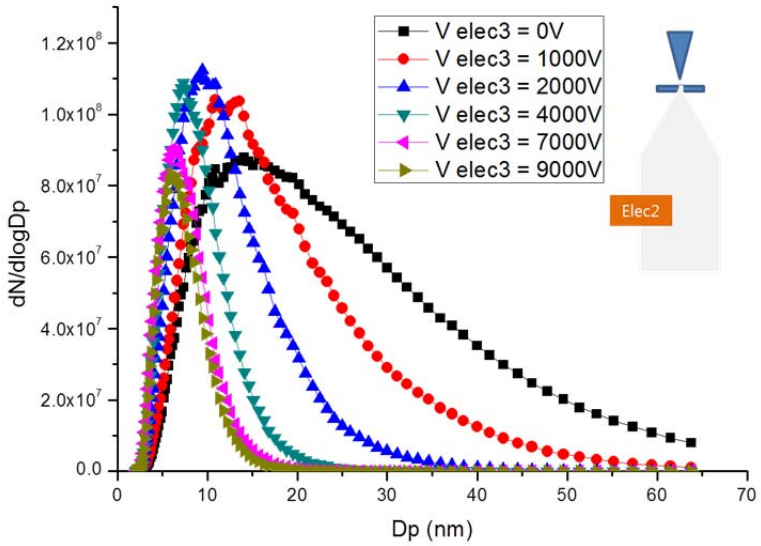

Figure 3.31. Total particle size distribution in Positive polarity E-field measure by SMPS (Lower port suction, electrode 2).

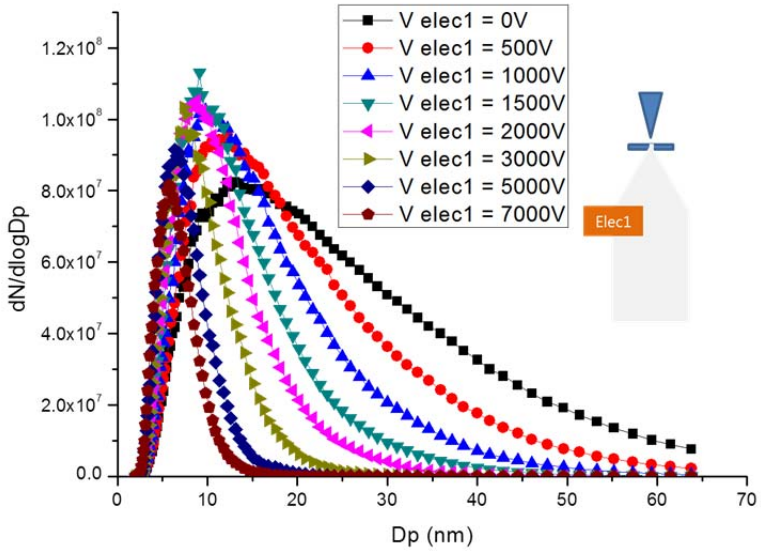

Figure 3.32. Total particle size distribution in Positive polarity E-field measure by SMPS (Lower port suction, <u>electrode 1</u>).

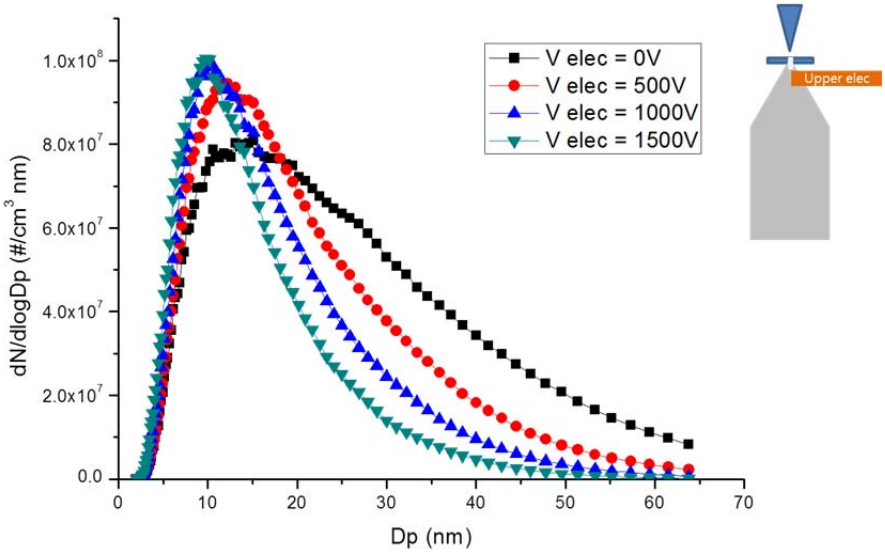

Figure 3.33. Total particle size distribution in Positive polarity E-field measure by SMPS (Lower port suction, <u>Upper electrode</u>).

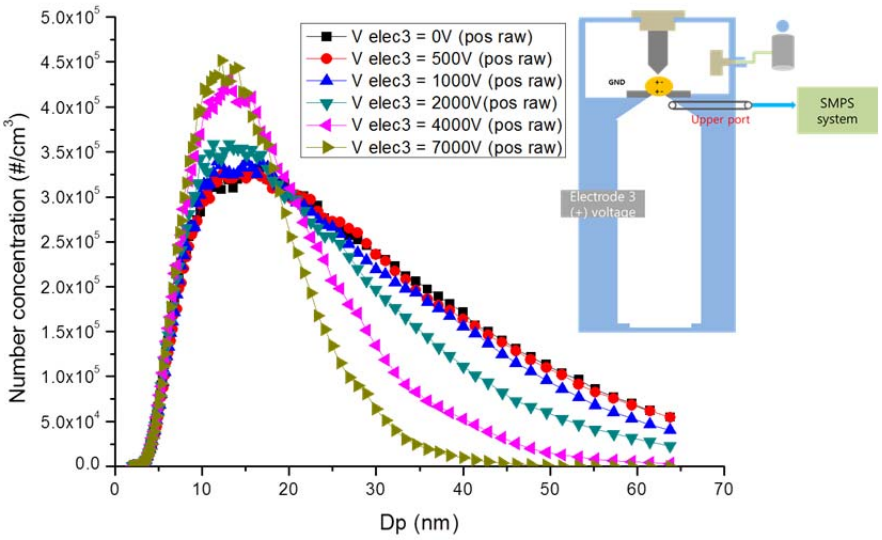

Figure 3.34. Positive particle size distribution in Positive polarity E-field measure by SMPS (<u>Upper port suction</u>, electrode 2).

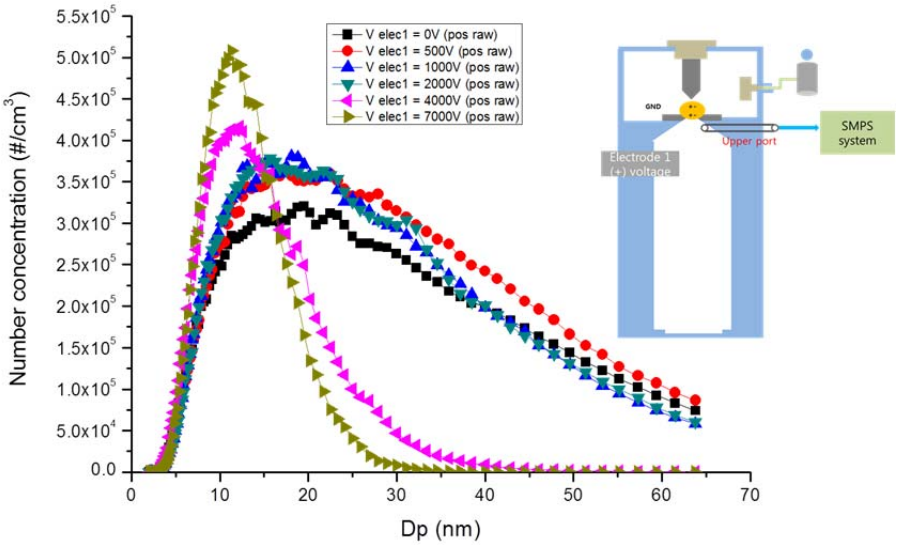

Figure 3.35. Positive particle size distribution in Positive polarity E-

field measured by SMPS (Upper port suction, electrode 1).

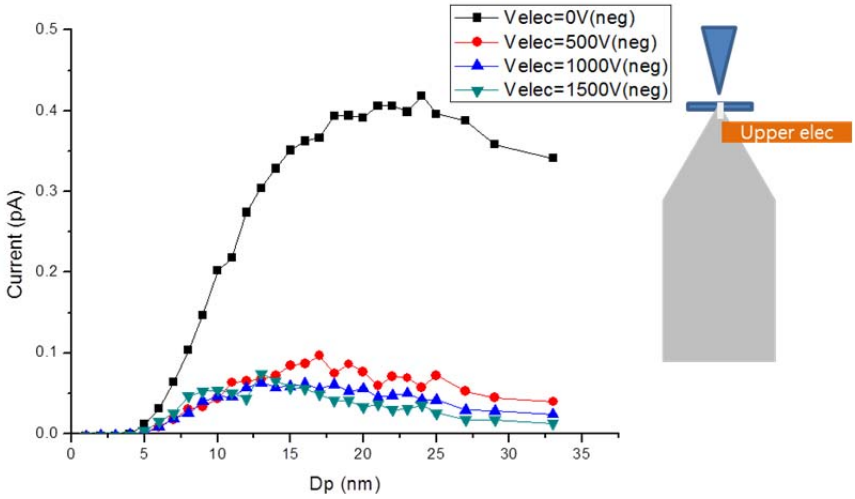

Figure 3.36. Negative particle size distribution in Positive polarity E-field measured by Electrometer (Lower port suction, Upper electrode).

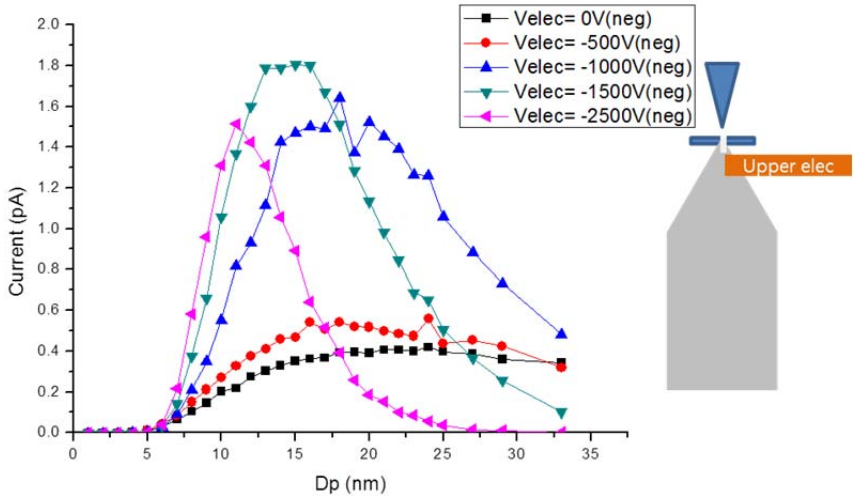

Figure 3.37. Negative particle size distribution in Negative polarity E-field measured by Electrometer (Lower port suction, Upper electrode).

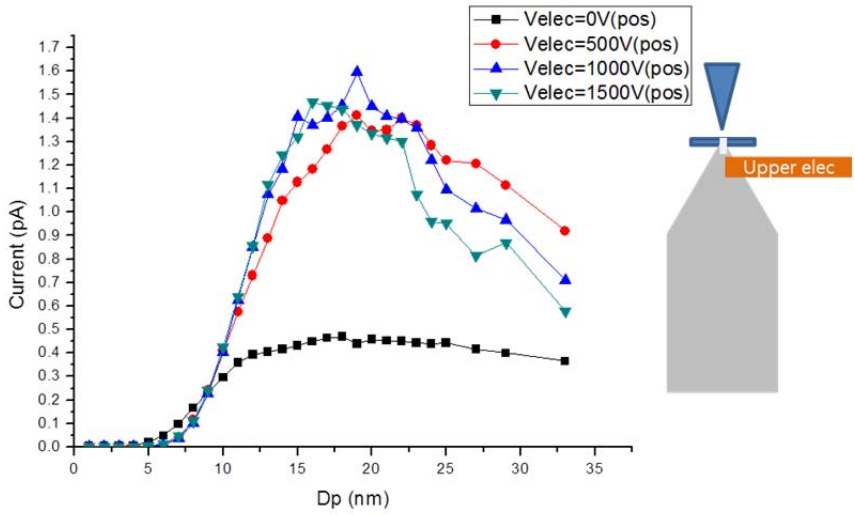

Figure 3.38. Positive particle size distribution in Positive polarity E-field measured by Electrometer (Lower port suction, Upper electrode).

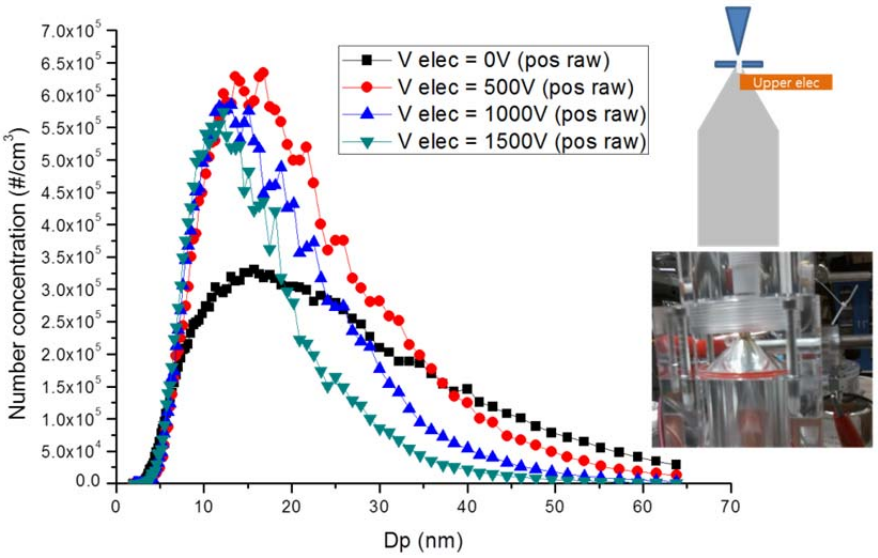

Figure 3.39. Positive particle size distribution in Positive polarity E-field measured by SMPS (Lower port suction, Upper electrode).

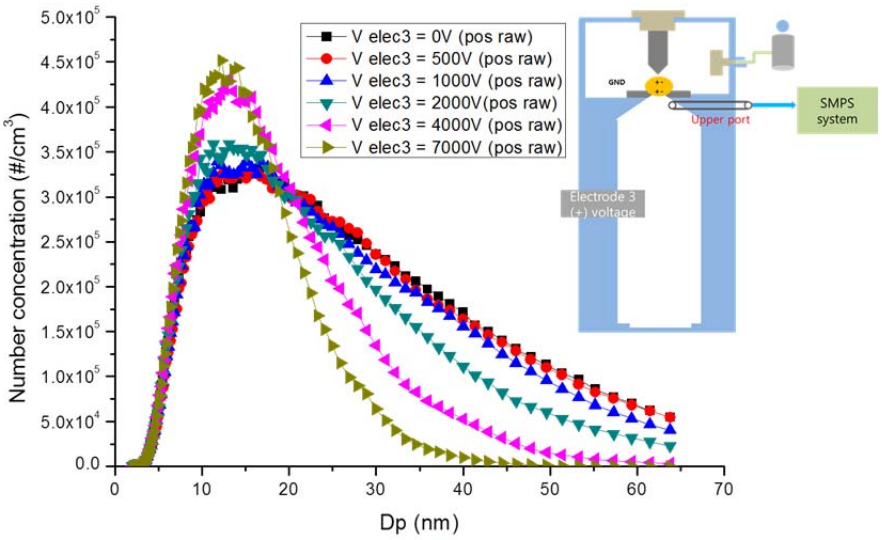

Figure 3.40. Positive particle size distribution in Positive polarity E-field measured by SMPS (Upper port suction, Electrode 2).

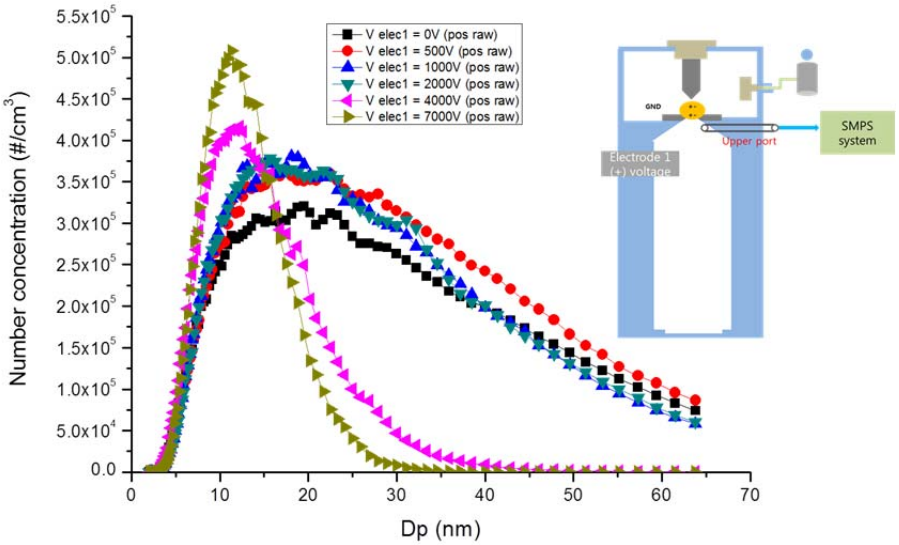

Figure 3.41. Positive particle size distribution in Positive polarity E-

field measured by SMPS (Upper port suction, Electrode 1).

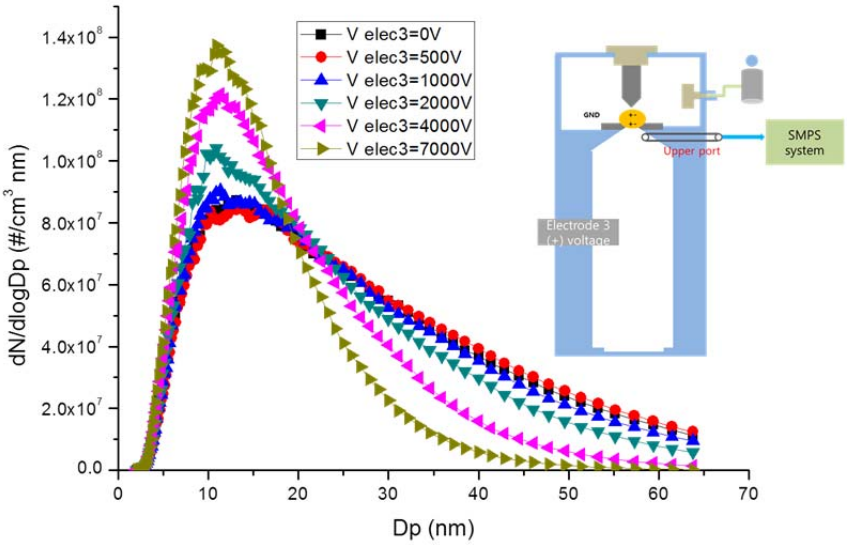

Figure 3.42. Total particle size distribution in Positive polarity E-field measured by SMPS (Upper port suction, Electrode 2).

3.4.3. Size seperation effect mechanism

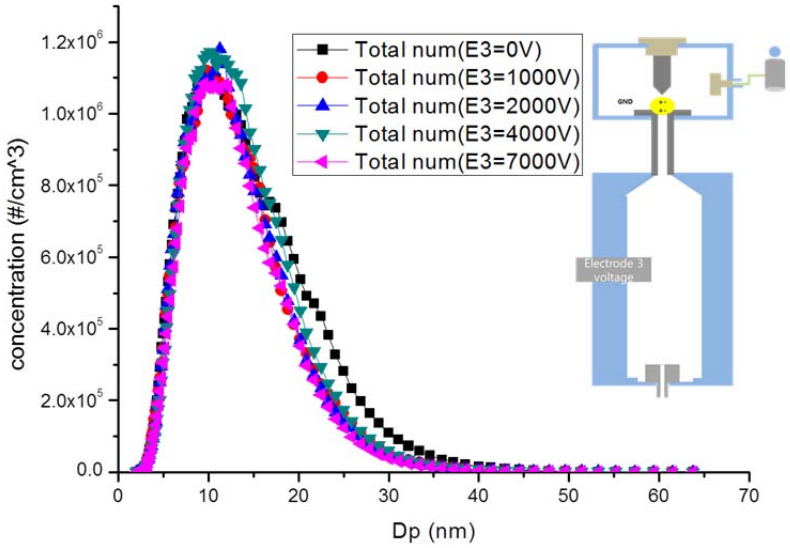

Figure 3.43. CSDG: Total particle size distribution in Positive polarity E-field measured by SMPS (Lower port suction, Electrode 2).

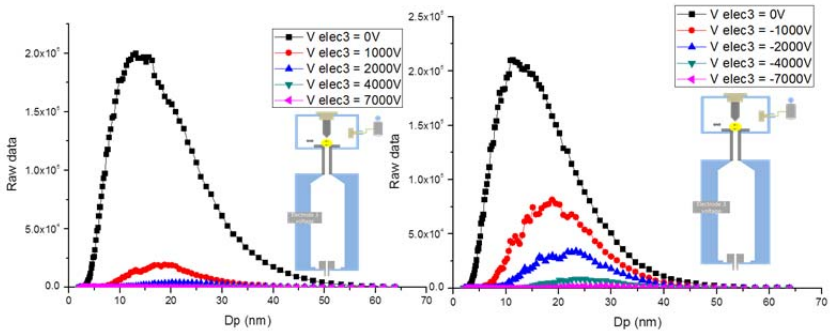

Figure 3.42. CSDG: Positive particle size distribution in Positive, negative polarities E-field measured by SMPS (Lower port suction, Electrode 2).

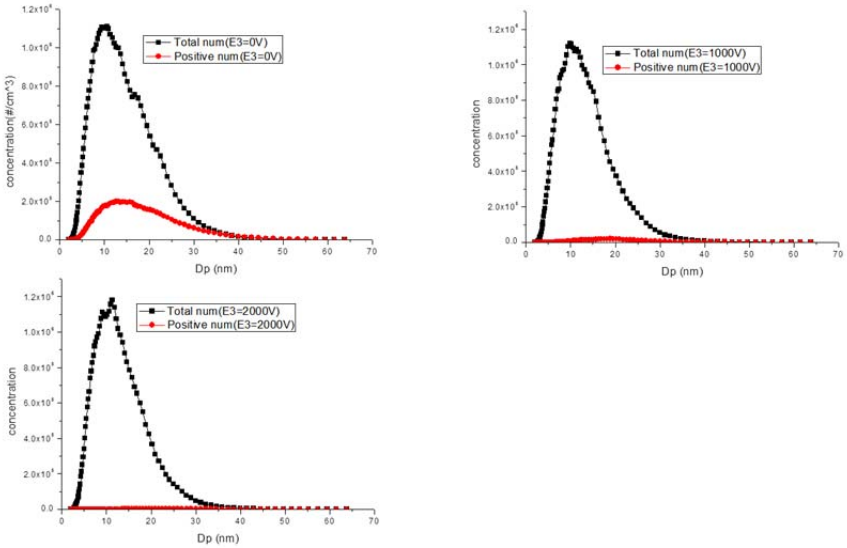

Figure 3.44. CSDG: Comparison fraction of total and positive particles.

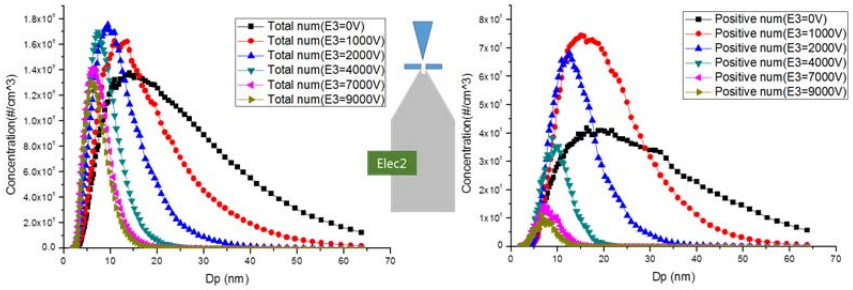

Figure 3.45. PSDM: Total, Positive particle size distribution in Positive polarity, E-field measured by SMPS (Lower port suction, Electrode 2).

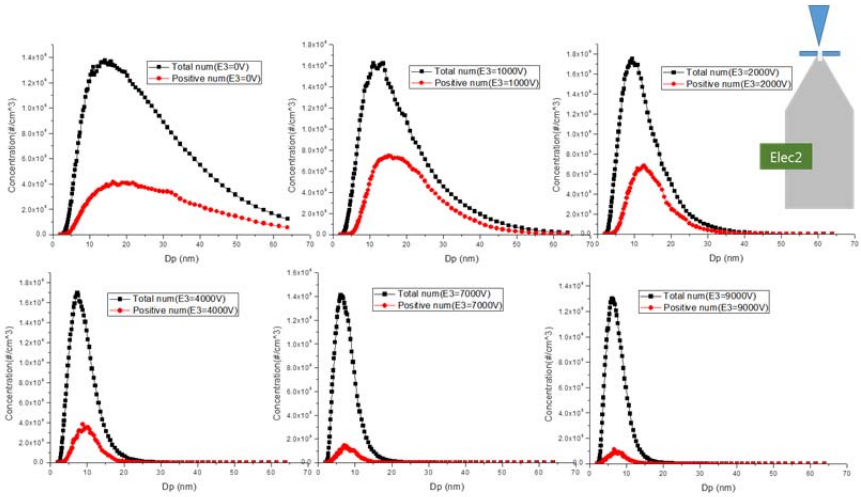

Figure 3.46. PSDM: Comparison fraction of total and positive particles.

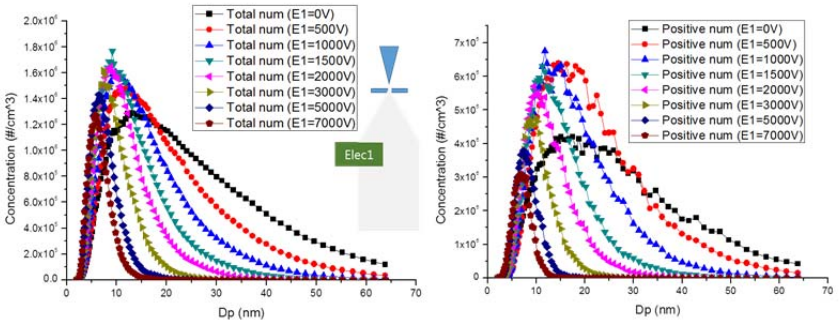

Figure 3.47. PSDM: Total, Positive particle size distribution in Positive polarity E-field measured by SMPS (Lower port suction, <u>Electrode 1</u>).

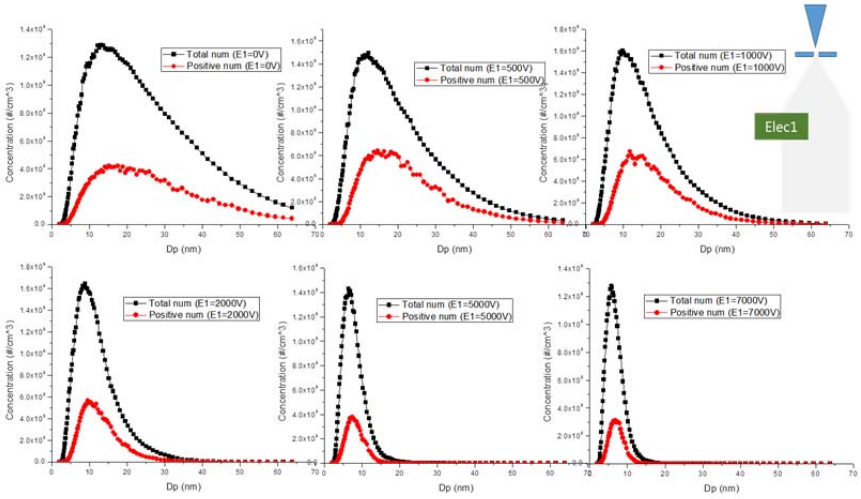

Figure 3.48. PSDM: Comparison fraction of total and positive particles. (Electrode 1)

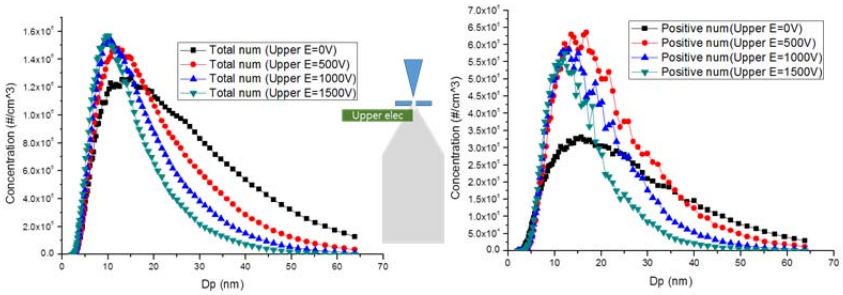

Figure 3.49. PSDM: Total, Positive particle size distribution in Positive, negative polarities E-field measured by SMPS (Lower port suction, Electrode 1).

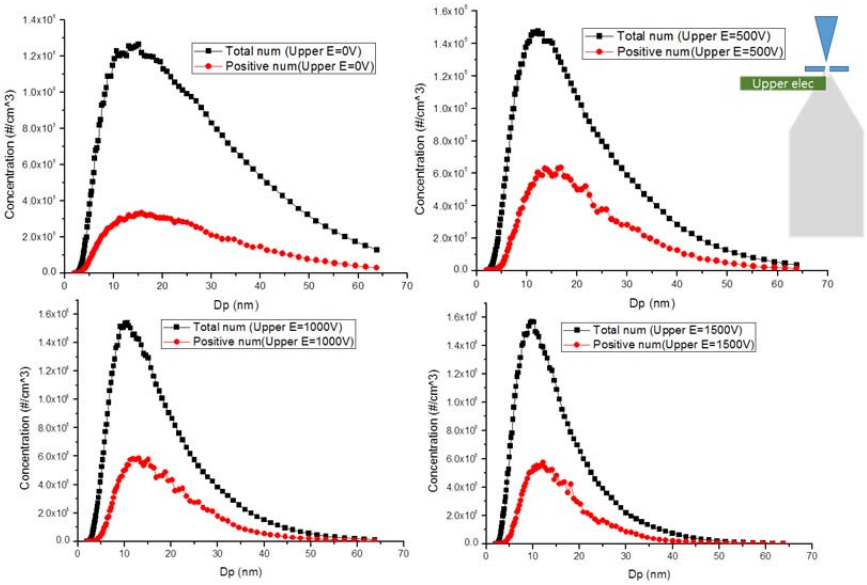

Figure 3.50. PSDM: Comparison fraction of total and positive particles.

(Upper electrode)

3.4.4. Stokes force and electric force

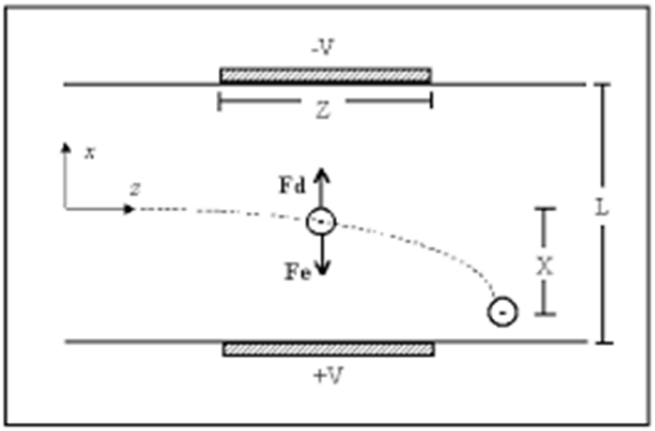

Figure 1: Deflection of a charged particle with charge Q in an electric field.

Figure 3.51. Interaction between stokes force and electric force

(Adopted from W.D.Marra Jr et al. 2000)

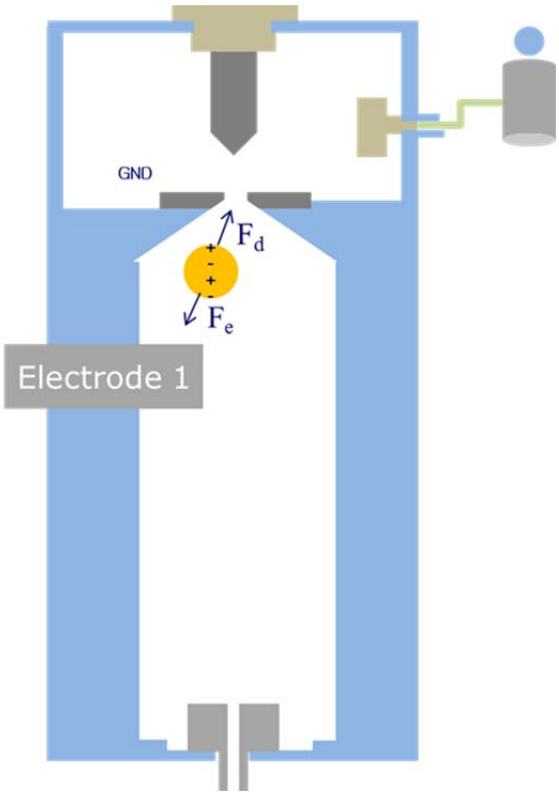

Figure 3.52. Interaction between stokes force and electric force in PSDM

To verify the post-spark plasma scenario against experiment quantitatively let us consider the motion of the polarized spherical plasma cloud as a whole in the non-uniform electric field of the rod-like electrode towards the electrode. If one considers the plasma cloud as a neutral ball of radius λ_p passing at distance R near the electrode, then the velocity of the cloud can be estimated from the balance equation of the Stokes force due to the dynamical ion viscosity μ_i and the electric force that drives the dipole moment of the cloud, induced by the external field, in the field gradient

$$6\pi\mu_i\lambda_p\vec{v_i} = \vec{\nabla}(\vec{d}\vec{E}), \qquad \textbf{[Equation 3.5]}$$

where the dipole moment of the cloud is $\vec{d} = {\lambda_p}^3\vec{E}$. Here we approximated the plasma cloud static polarizability by the cube of its radius assuming the conductive plasma ball.

3.4.5. Determining the critical radius of particle (F_e=F_i)

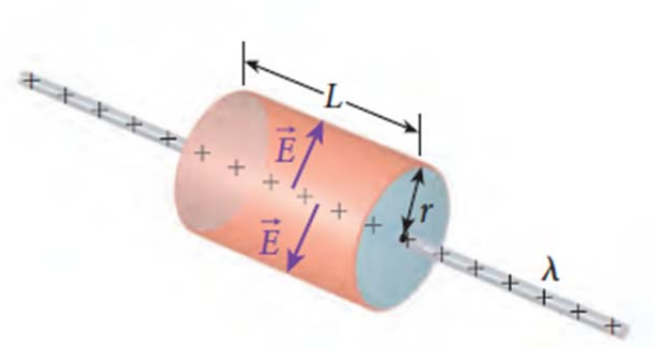

Figure 3.53. Electric field of a rod-like electrode

(Adopted from "Electric fields and Gauss's law.pdf")

$$\oiint \vec{E} \bullet d\vec{A} = EA = E\left(2\pi rL\right) = \frac{q}{\epsilon_0} = \frac{\lambda L}{\epsilon_0}$$

$$E = \frac{\lambda}{2\pi\epsilon_0 r} = \frac{2k\lambda}{r}$$

$$\partial E = \frac{\partial V}{\partial R},\ \partial V = \partial E \partial R,\ V = \int_{R_0}^{R} E\ \partial R = \int_{R_0}^{R} \frac{2\lambda}{R}\ \partial R = 2\lambda(\ln\frac{R}{R_0}) + V_0 \approx 2\lambda,\ E \approx \frac{V}{R}$$

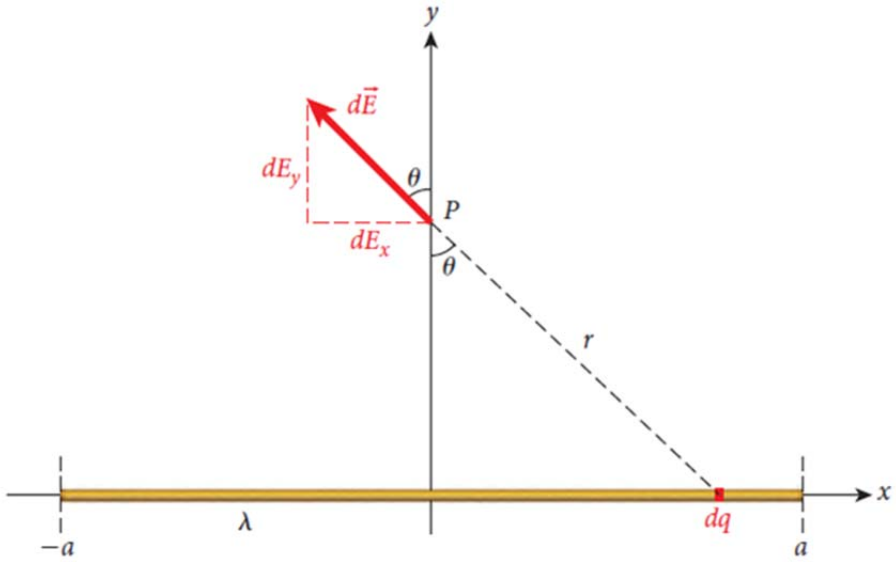

Figure 3.54. Electric field of a rod-like electrode another approach

(Adopted from "Electric fields and Gauss's law.pdf")

$$E_y = 2\int_0^a dE_y = 2\int_0^a k\frac{dq}{r^2}\cos\theta = 2k\int_0^a \frac{\lambda dx}{r^2}\frac{y}{r} = 2k\lambda y\int_0^a \frac{dx}{\left(x^2+y^2\right)^{3/2}}.$$

$$\int_0^a \frac{dx}{\left(x^2+y^2\right)^{3/2}} = \left[\frac{1}{y^2}\frac{x}{\sqrt{x^2+y^2}}\right]_0^a = \frac{1}{y^2}\frac{\boldsymbol{a}}{\sqrt{y^2+a^2}}.$$

$$E_y = 2k\lambda\, y\frac{1}{y^2}\frac{a}{\sqrt{y^2+a^2}} = \frac{2k\lambda}{y}\frac{a}{\sqrt{y^2+a^2}}$$

$$E_y = \frac{2k\lambda}{y}. = \frac{2\lambda}{r}$$

The field of a rod-like electrode (a charged cylinder) can be estimated as

$$\left|\vec{E}\right| = V/R \qquad \textbf{[Equation 3.6]}$$

where V is the electrode potential. By combining Eqs. (4) and (5) we obtain

$$|\vec{v_i}| = \frac{1}{3\pi\mu_i}\frac{{\lambda_p}^2}{R^3}V^2 \qquad \textbf{[Equation 3.7]}$$

3.4.6. Definition of a new law (dipole parameter $\equiv Vr_d{}^2$)

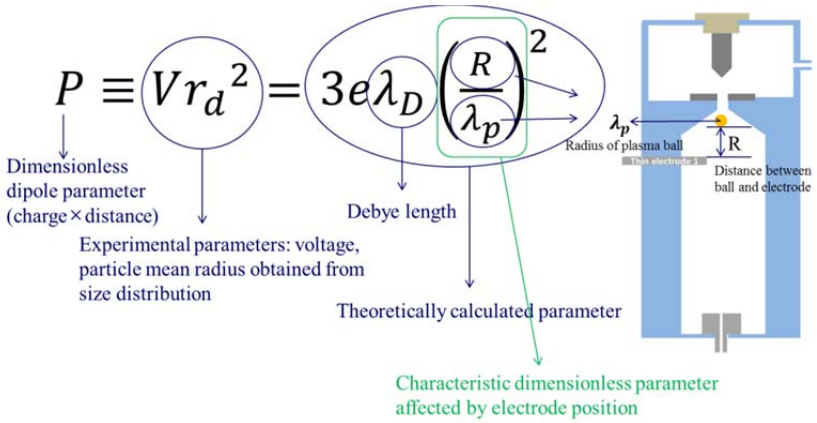

Figure 3.55. Parameters definition of central equation *P*

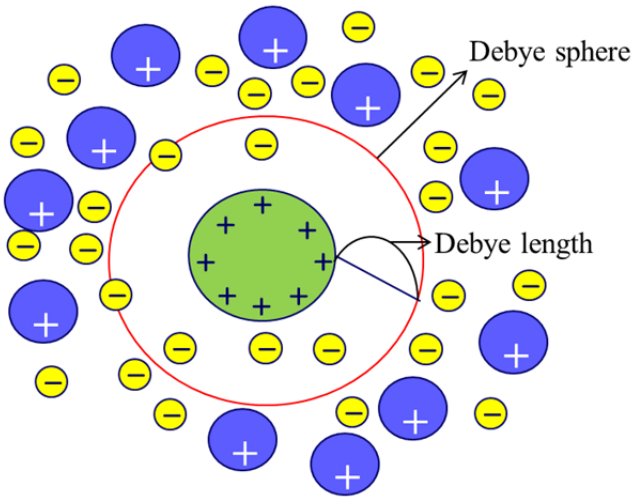

Figure 3.56. Concept of Debye length

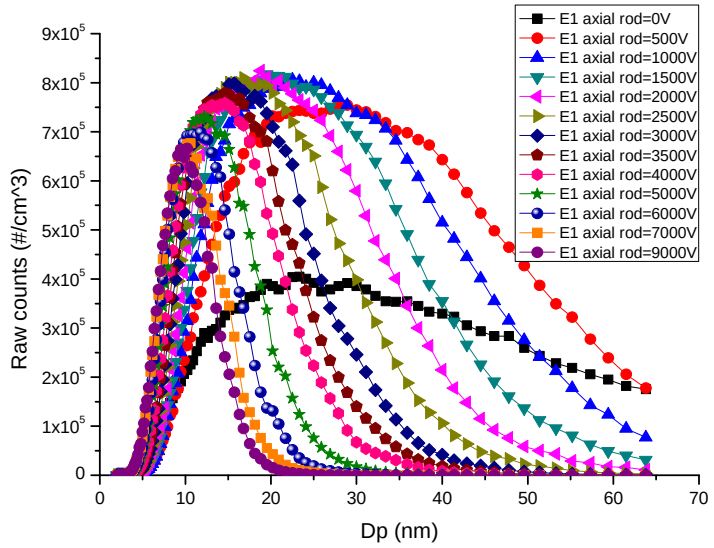

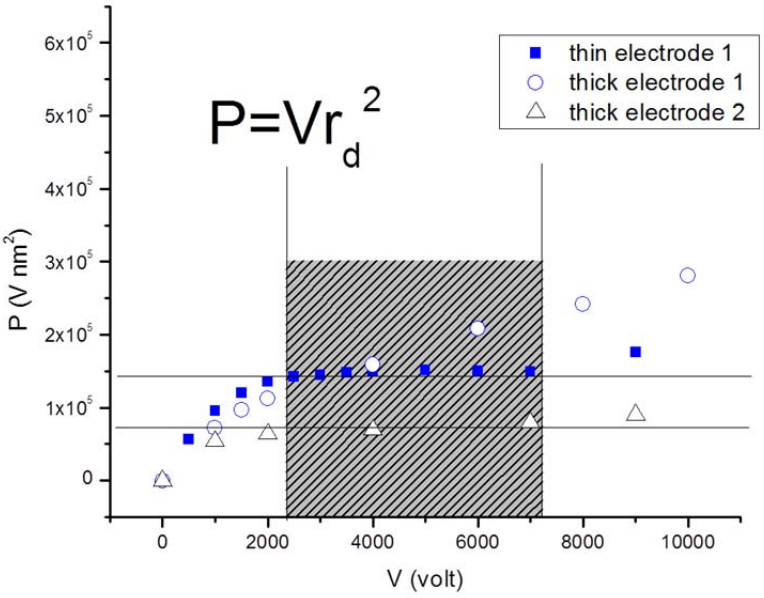

Figure 3.57. "Dipole" parameter *P* calculated from experimental PDFs for positively charged particles for different external fields for three field

configurations. The straight lines illustrate the constant *P* as the prediction of this theory.

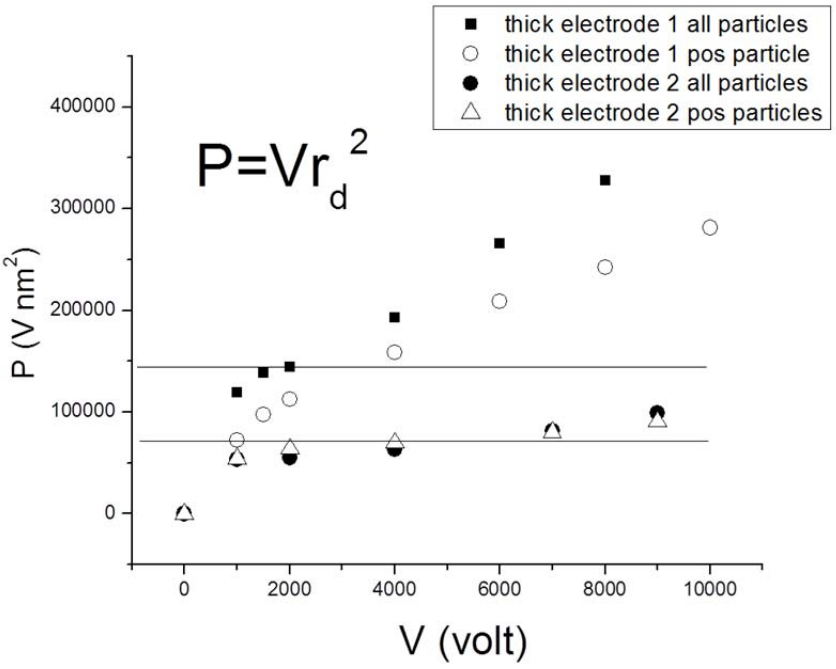

Figure 3.58. Comparison of *P* for all particles with *P* for positive particles in case of thick electrodes.

$\overrightarrow{F_{ion}} = \overrightarrow{F_{collision}} + \overrightarrow{F_{orbital}} \sim \overrightarrow{F_{collision}}$

$\overrightarrow{F_{collision}} = n_i v_s m_i \vec{v_s} \pi {b_c}^2 \propto (particle\ radius)^2$

$\overrightarrow{F_{orbital}} = n_i v_s m_i \vec{v_s} 4\pi {b_{\pi/2}}^2 \Gamma \propto (particle\ charge)^2$

Orbital or coulomb force

$$b_c^2 = a^2(1 - \frac{2e\varphi_f}{m_i v_s^2})$$

$$b_{\pi/2}^2 = \frac{Qe}{4\pi\epsilon_0 m_i v_s^2}$$

$$\vec{F_i} = n_i v_s m_i \vec{v_i} \pi {r_d}^2 \qquad \textbf{[Equation 3.5]}$$

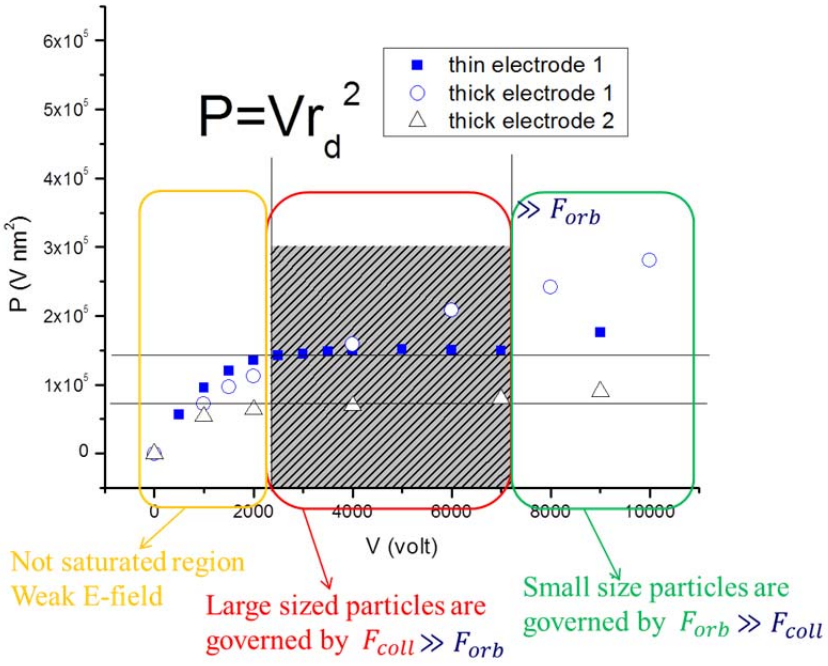

Figure 3.59. Three region about Dipole" parameter *P*.

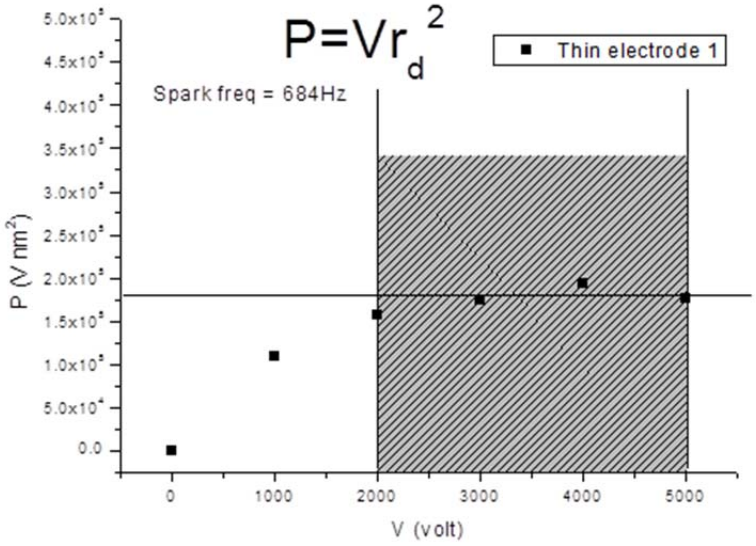

Figure 3.60. Dipole" parameter *P* calculated from experimental PDFs for high spark frequency (684Hz) case.

Finally, equating forces from Eqs. (2) and (3) to determine the particle radius below which the particle can overcome the ion drag force and be expelled by the field from the cloud with taking account of Eq. (6) we get

$$P \equiv V{r_d}^2 = \frac{3e\eta_i}{v_s}\left(\frac{R}{\lambda_p}\right)^2 = 3e\lambda_D\left(\frac{R}{\lambda_p}\right)^2 \qquad \textbf{[Equation 3.7]}$$

where the ion kinematic viscosity $\eta_i = \mu_i/m_i n_i$ can be estimated as $\eta_i = v_s\lambda_D$ with the Debye length $\lambda_D = \sqrt{T_i/(4\pi e^2 n_i)}$ (Bonitz et al. 2010). Constant P from Eq. (3.7) has the dimension of the dipole moment and can be found from experimental data for thick/thin electrode 2 (see Fig.. 2.7) $P \approx 0.8 \times 10^5 Vnm^2 \approx 0.27 \times 10^7 D$ ($1D = 1 \times 10^{-18} esu\ cm$).

On the other hand, $\lambda_D \approx 3.8 \times 10^{-6} cm$ for $n_i \approx 10^{15} cm^{-3}$ and the right hand side of Eq. (3.7) takes nearly the same value if, for example, $R \approx 10 cm$ and $\lambda_p \approx 0.5 cm$. Additionally, for the same parameters Eq. (6) gives an acceptable estimate $|\vec{v_i}| \approx 3 \times 10^4 cm/sec$ at $V \approx 900\, V$, $m_i \approx 0.47 \times 10^{-22} g$, $v_s \approx 6 \times 10^4 cm/sec$ provided the simplicity of our approach.

Equation 3.7 is the central result of this research. As one can see from Fig.3.56 the product $P = V r_d{}^2$ being determined from experimental PDFs (see for example Fig. 3.56 and Fig. 3.57) is a constant in a wide range of voltage with sufficient accuracy for thin electrode 1,2 and thick electrode 2, provided an approximate character of our theory. We took for r_d the mean radius determined from the PDF using the fact that the PDF considerably narrows with the voltage. In case of thick electrode 1 where the field gradient is the least of all other cases, because the electrode thickness is comparable with the distance to the other electrodes and thick electrode 1 has broad flat butt (Fig. 2.6) reducing the field gradient, therefore its size separation capacity quickly saturates with voltage (see below), that is r_d stops varying with voltage at larger values and P becomes proportional to V. Still, the constant P is not universal and depends on a chamber configuration as is seen from Fig. 3.57. Namely, for electrode 2 that is located twice father downstream from the discharge gap than electrode 1 the constant is two times lower according to Fig. 3.57. Parameter P is also

relevant for the mean radius defined from the PDF of all nanoparticles (not only positive) and has the same value as is seen from the data shown in Fig.. 2.6 b for the thick electrode 2 (see the PDFs for this case in Fig.. 3.57). This happens because a portion of positive nanoparticles was neutralized in plasma and contributed to neutral nanoparticles.

Note that the ion drag force also contains the Coulomb-collision part (Barnes et al. 1992) that for particles of unit charge is characterized by a particle-size-independent small scale length parameter $b_{\pi/2}$ (the impact parameter whose asymptotic orbit angle is $\pi/2$) which plays role only at larger voltages when PDF itself shifts to the smaller sizes (Fig.. 2.6b). At some large voltage the PDF stops changing (r_d stops changing as well) and thus the parameter P starts growing with the voltage as is seen in Fig. 2.6a.

3.5. Conclusion

In order to consider the effect of electric field, the simulation on the electric field strength in the connection tube region of the PSDM and the CSDG was accurately carried out. It is expected that particles generated immediately after spark discharge are affected by electric field in the PSDM contrary to the CSDG. For investigating the electric field effect in connection tube region, we have developed a rigorous theory that explains the underlying mechanism of particle size selection and formulates a novel law relating the average particle size with the voltage applied. Our analysis about the mechanism presents that as the dust particles are charged, the plasma can exhibit many new phenomena directly linked to the dust particles. The phenomenon of the influence of the electric field on the particle size distribution arise from the attraction of the plasma cloud to the electrode and in the difference in the coupling to plasma for large and small radius particles. Through this mechanism analysis, it is expected that if voltage, i.e., electric field intensity is increased, smaller charged particles are alive more and then particle size distribution function moves towards smaller particle sizes.

In summary, we have demonstrated that the particles size distribution in residual spark discharge plasma can be controlled by the non-uniform external electric field separating small and large nanoparticles due to the ion drag force that sweeps away larger particles along with the plasma cloud. The theory predicts that the product of the electrode voltage and the square

of the mean particle radius be a constant which is confirmed by the experiment. The external electric field as a new controlling parameter can replace the gas flow control and this may be of great importance for nano-pattern applications.

3.6. References

Barnes, M., Keller, J., Foster, J., O'Neill, J. and Coutlas,D. (1992). Phys. Rev. Lett. **68**, 313

Bengt O. Meuller , Maria E. Messing , David L. J. Engberg , Anna M. Jansson , Linda I. M. Johansson , Susanne M. Norlén , Nina Tureson , and Knut Deppert. (2012). Aerosol Sci.Tech., **46**, 1256

Bonitz, M., Horing, N., Ludwig, P. (2010). *Introduction to Complex Plasma*, Springer-Verlag, Berlin, Heidelberg

Borra, J.(2006). J. Phys. D: Appl. Phys. **39**, R19

Choi,H.,Kang,S.,Jung,W.,Jung,Y.,Park,S.,Kim,D.,&Choi,M.(2015). Controlled electrostatic focusing of charged aerosol nanoparticles via an electrified mask. *Journal of Aerosol Science*, 88, 90-97.

Ha, K., Choi, H., Jung, K., Han, K., Lee, J. K., Ahn, K., & Choi, M. (2014). Large-area assembly of three-dimensional nanoparticle structures via ion assisted aerosol lithography with a multi-pin spark discharge generator. *Nanotechnology, 25*(22), 225302. doi: 10.1088/0957-4484/25/22/225302

Han, K., Kim, W., Yu, J., Lee, J., Lee, H., Gyu Woo, C., & Choi, M.(2012). A study of pin-to-plate type spark discharge generator for producing unagglomerated nanoaerosols. *Journal of Aerosol Science, 52*, 80-88. doi: 10.1016/j.jaerosci.2012.05.002

Kim,H.,Kim,J.,Yang,H.,Suh,J.,Kim,T.,Han,B.,Kim,S.,Kim,D.,Pikhitsa,PV.,&

Choi,M.(2006).Parallel patterning of nanoparticles via electrodynamic focusing of charged aerosols. Nature *Nanotechnology*, 1, 117–121.

Kim,W., Pikhitsa,PV. and Choi,M. (2016). Particle size selection in post-spark dusty plasma in non-uniform electric field. *Applied Physics Letter*

Lee,H.,You,S.,Pikhitsa,PV.,Kim,J.,Kwon,S.,Woo,CG.,&Choi,M.(2011).Thre e-dimensional assembly of nanoparticles from charged aerosols. *Nano Letters*, 11, 119–124.

Ludvigsson, L., Meuller, B. and Messing, M.(2015). Investigations of initial particle stages during spark discharge. J. Phys. D: Appl. Phys. 48, 314012

Maxime Mikikian, Marjorie Cavarroc, Lénaïc Couëdel, Yves Tessier, and Laïfa Boufendi, Pure Appl. Chem., **82**, 1273 (2010)

Park, K.-T., Farid, M. M., & Hwang, J. (2014). Anti-agglomeration of spark discharge-generated aerosols via unipolar air ions. *Journal of Aerosol Science*, *67*, 144-156.

Schwyn,S.,Garwin,E.,&Schmidt-Ott,A.(1988).Aerosol generation by spark discharge. *Journal of Aerosol Science*, 19, 639–642.

Sung,H.,Lee,J.,Han,K.,Lee,J.-K.,Sung,J.,Kim,D.,Choi,M.,Kim,C.(2014)

Controlled positioning of metal nanoparticles in an organic light-emitting device for enhanced quantum efficiency. *Organic Electronics*, 15(2),491-499.

Tabrizi,N.,Ullmann,M.,Vons,V.,Lafont,U.,&Schmidt-Ott,A.(2009a).

Generation of nanoparticles by spark discharge. *Journal of Nanoparticle*

Research, 11, 315–332.

Zafiu, C., Melzer, A. and Piel, A.(2003). Physics of Plasmas., **10**, 5

Sukhinin, G., Fedoseev, A., Khokhlov, R. and Suslov, R. (2012). Contrib. Plasma Phys. **52**, 62

This page is intended to be blank

Chapter 4.

Applications for three dimensional nanostructure fabricated via spark discharge

4.1. Introduction

Charged nanoparticles generated by spark discharge can be used to nanostructure patterning (choi et al., 2015, kim et al., 2006, Lee et al., 2010, Ha et al., 2014). Also recent study present that they can be used to renewal energy device (Ha et al., 2016). But there exists a problem being generated large particles during spark discharge process. If these large particles generated due to instability of spark are deposited a layer in energy device such as solar cell, the short current flows through the device and then it destroys the device. Large particles or agglomerates should be eliminated to solve this problem. Also since there needs much amounts of particles to deposit in large area patterned device, spark frequency must be high. And it needs high gas flow rate condition to prevent agglomeration among the much amounts of charged particles (Noh et al.,2016, Ha et al., 2014). However there are restrictions as to too high flow rates that blow the particles away of their trajectories along the electric field lines during the patterning procedure[4] or spark discharge instabilities occurring at large frequencies.

Motivated by this, Electric field effect could be applied to fabricate well-patterned 3D nanoparticle structures while preventing agglomeration and generating a lot of small charged particles in low gas flow rate condition.

4.2. Background and Experimental Procedure

4.2.1. Single pin spark chamber

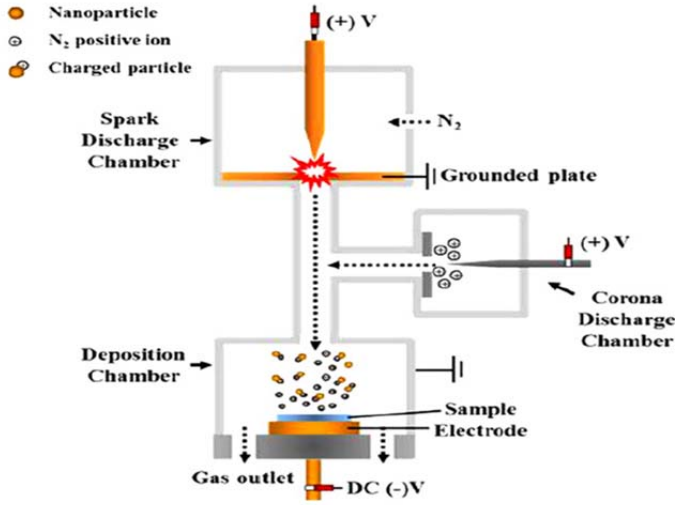

Figure 4.1. Schematics of IAAL with a single-pin SDG. (Adopted from Ha et al. 2014)

4.2.2. Multi pin spark chamber

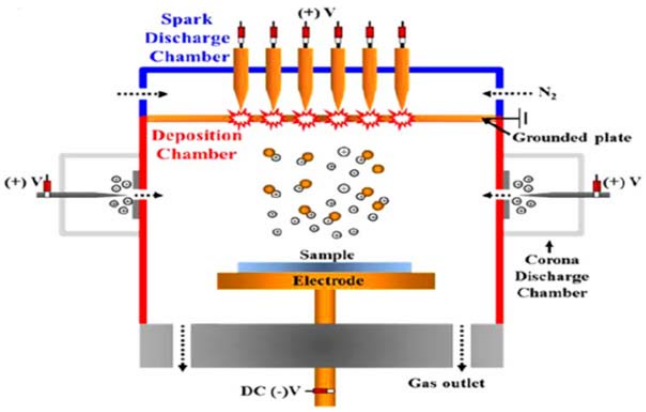

Figure 4.2. Schematics of IAAL with a multi-pin SDG. (Adopted from Ha et al. 2014)

4.3. Results and Discussions

4.3.1. The effect of large nano-cluster elimination

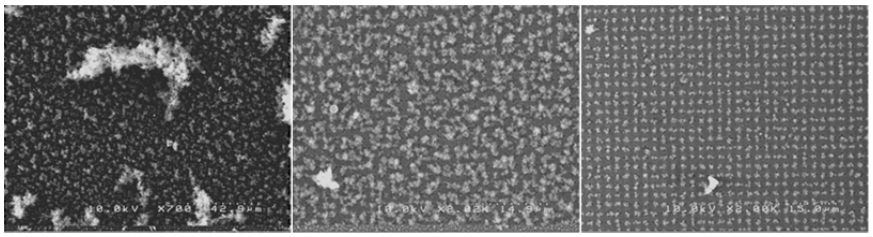

V= 0V **V=1500V** **V=4000V**

Figure 4.3. 3D structures array of Cu nanoparticles fabricated on a Si-substrate (5 mm × 5 mm size). Voltage of the (a) EF electrode = 0V, (b) 1500V, and (c) 4000V.

The PSDM could be applied to manufacture three dimensional (3D) nanostructures. It is possible to prevent agglomeration, because large particles could be eliminated by applied electric field. Figure 4.3 shows how the electric field affects to fabricate three dimensional nanoparticle structures while maintaining the other factors the same such as spark repetition frequency, energy per spark, gas flow rate, etc. Large agglomerates were eliminated and the particle size was decreased as voltage of the EF electrode increased. Therefore, well-patterned nanostructures were fabricated by using the PSDM as shown in Fig. 4.3(c). It is expected that the PSDM could be utilized to prevent agglomeration fundamentally through controlling the post spark discharge regime.

4.3.2. Increase of number, volume concentration of nanoparticles

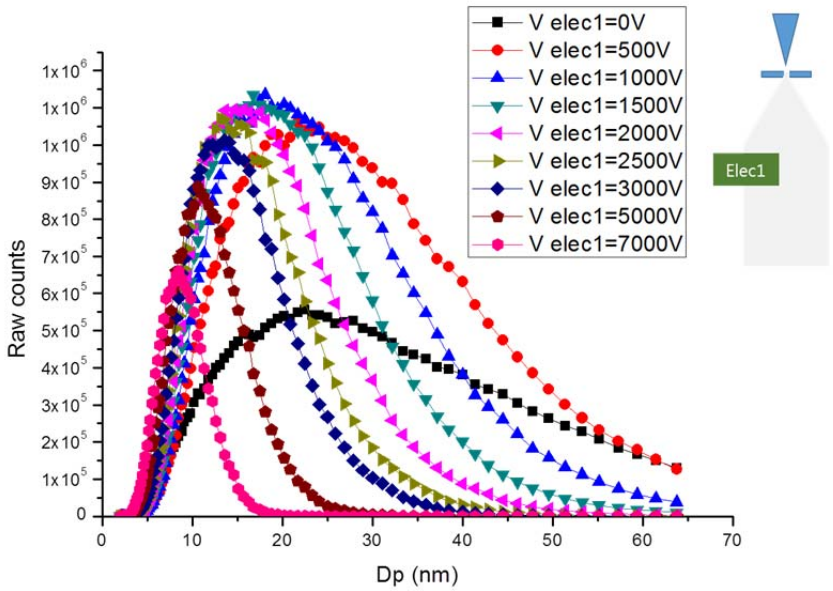

Figure 4.4. PSDM: Positive particle size distribution in Positive polarity E-field measured by SMPS (Lower port suction, Electrode 1).

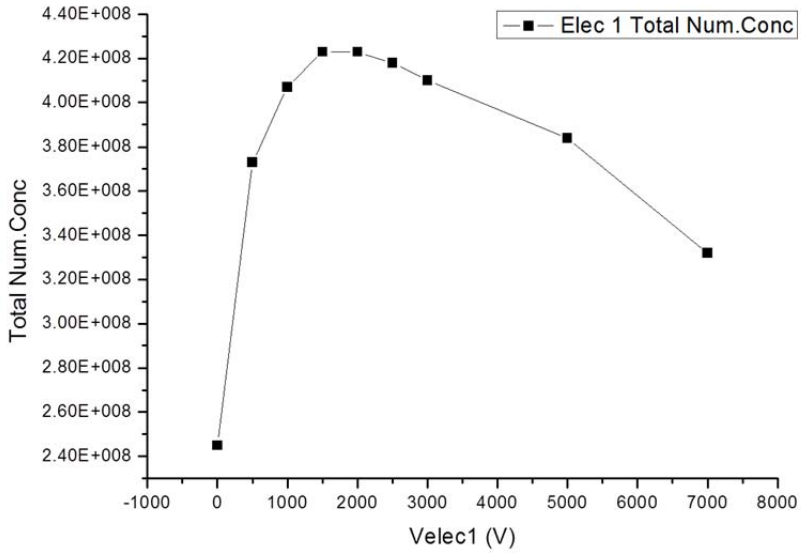

Figure 4.5. Total number concentration (electrode 1)

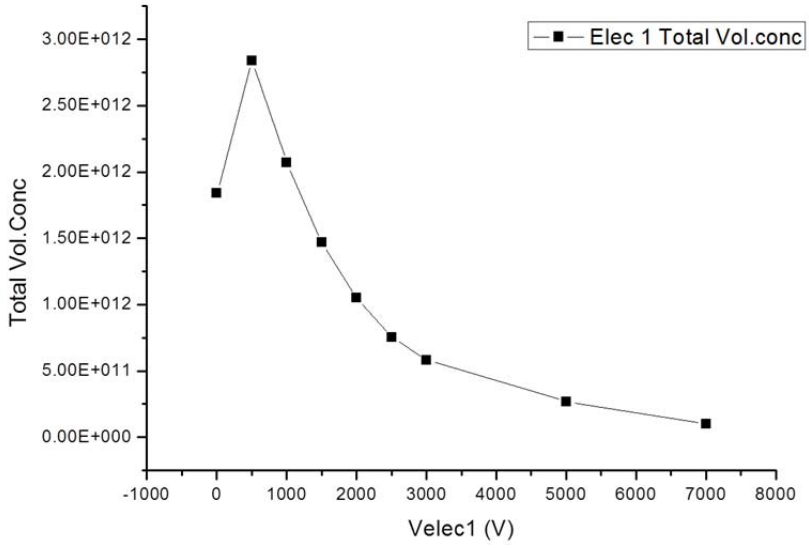

Figure 4.6. Total volume concentration (electrode 1)

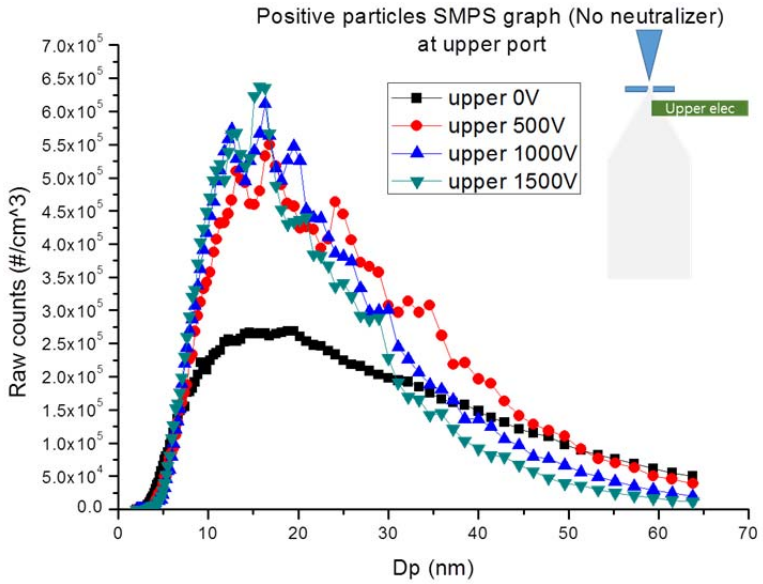

Figure 4.7. PSDM: Positive particle size distribution in Positive polarity E-field measured by SMPS (Lower port suction, Upper electrode).

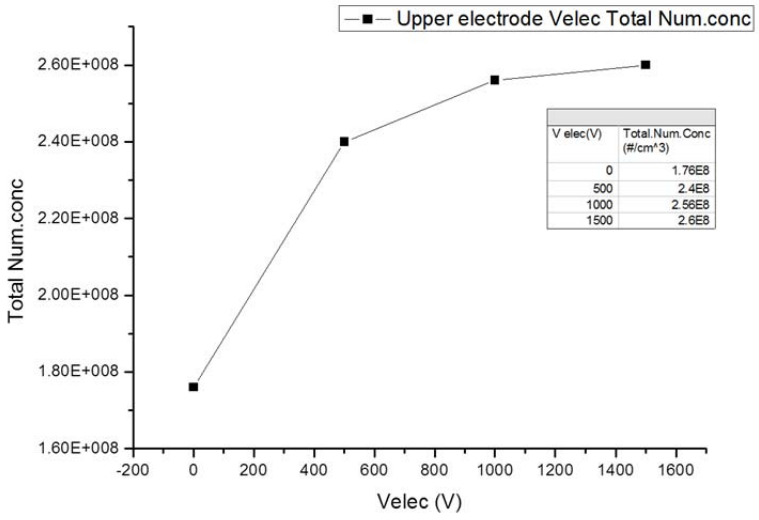

Figure 4.8. Total number concentration (upper electrode)

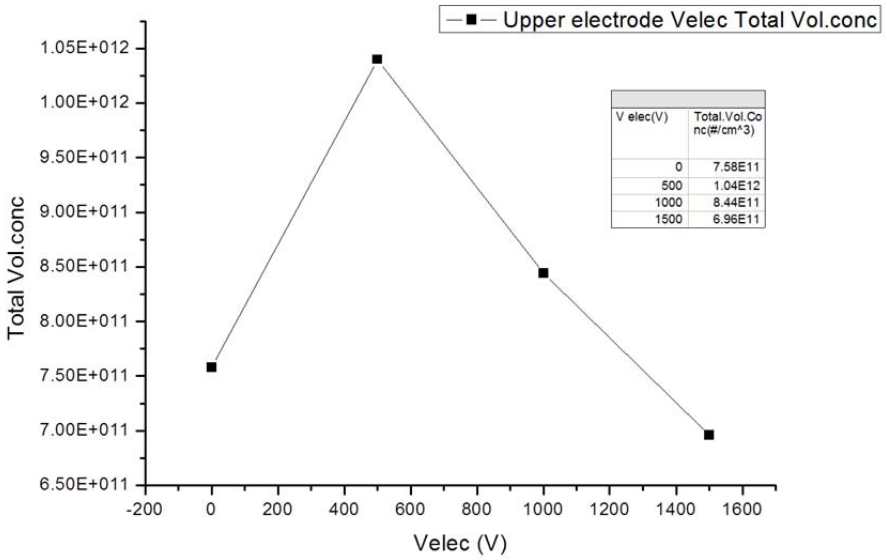

Figure 4.9. Total volume concentration (upper electrode)

4.4. Conclusion

While maintaining the other factors the same such as spark frequency, spark energy, gas flow, etc, this technology was applied to fabricate three dimensional (3D) nanoparticle structures in large area substrate (5 mm × 5 mm size). When voltage of EF electrode was increased, large agglomerates were eliminated and the size of particles was decreased, so well-patterned nanostructures were fabricated.

Furthermore, large amounts of charged particles could be obtained by controlling the electric field. Their number and volume concentration increased according to electric potential in low voltage area. Also this post spark discharge manipulator can be utilized to high frequency spark discharge process because of low gas flow rate condition.

4.5. References

Bau,S.,Witchger,O.,Gensdarmes,F.,Thomas,D.,&Borra,J.-P.(2010). Electrical properties of airborne nanoparticles produced by a commercial spark-discharge generator. *Journal of Nanoparticle Research*, 12, 1989–1995.

Biskos,G.,Vons,V.,Yurteri,C.,&Schmidt-Ott,A.(2008). Generation and sizing of particles for aerosol-based nanotechnology. *KONA PowderParticle Journal*, 26, 13–35.

Choi,H.,Kang,S.,Jung,W.,Jung,Y.,Park,S.,Kim,D.,&Choi,M.(2015). Controlled electrostatic focusing of charged aerosol nanoparticles via an electrified mask. *Journal of Aerosol Science*, 88, 90-97.

Evans,D.E.,Harrison,R.M.,&Ayres,J.G.(2003).The generation and characterisation of elemental carbon aerosols for human challenge studies. *Journal of Aerosol Science*, 34, 1023–1041.

Horvath,H.,&Gangl,M.(2003).A low-voltage spark generator for production of carbon particles. *Journal of Aerosol Science*, 34, 1581–1588.

Roth C, Ferron GA, Karg E, Lentner B, Schumann G,Takenaka S, Heyder J (2004) Generation of ultrafine particles by spark discharging. *J Aerosol Sci Technol* 38, 228–235Tabrizi,N.,Xu,Q.,vanderPers,N.,&Schmidt-Ott,A.(2010).Generation of mixed metallic nanoparticles from immiscible metals by spark discharge. *Journal of Nanoparticle Research*, 12, 247–259.

This page is intended to be blank

Chapter 5.
Concluding Remarks

We developed the new spark discharge generator able to prevent agglomeration and generate a large amount of charged particles via controlling the post spark regime. As a result, it was found that the post spark discharge manipulator (PSDM) was an effective device to prevent agglomeration and generate a large amount of charged particles. Unagglomerated and positively charged particles were produced through the PSDM chamber due to the electric field effect. In addition, the size and amount of neutral particles changed surprisingly as well as that of charged particles changed by the electric field. Thus, it is apparent that electric field played an important role in the PSDM. After developing the PSDM, it could be applied to manufacture three dimensional nanostructures. As a result, well-patterned nanostructures were fabricated by using the PSDM. Therefore, it is expected that the PSDM could be utilized to prevent agglomeration fundamentally through controlling the post spark discharge regime.

In order to consider the effect of electric field, the simulation on the electric field strength in the connection tube region of the PSDM and the CSDG was accurately carried out. It is expected that particles generated immediately after spark discharge are affected by electric field in the PSDM contrary to the CSDG. For investigating the electric field effect in connection tube region, we have developed a rigorous theory that explains the underlying mechanism of particle size selection and formulates a novel law relating the average particle size with the voltage applied. Our analysis about the mechanism presents that as the dust particles are charged, the plasma can

exhibit many new phenomena directly linked to the dust particles. The phenomenon of the influence of the electric field on the particle size distribution arise from the attraction of the plasma cloud to the electrode and in the difference in the coupling to plasma for large and small radius particles. Through this mechanism analysis, it is expected that if voltage, i.e., electric field intensity is increased, smaller charged particles are alive more and then particle size distribution function moves towards smaller particle sizes.

In summary, we have demonstrated that the particles size distribution in residual spark discharge plasma can be controlled by the non-uniform external electric field separating small and large nanoparticles due to the ion drag force that sweeps away larger particles along with the plasma cloud. The theory predicts that the product of the electrode voltage and the square of the mean particle radius be a constant which is confirmed by the experiment. The external electric field as a new controlling parameter can replace the gas flow control and this may be of great importance for nano-pattern applications.

While maintaining the other factors the same such as spark frequency, spark energy, gas flow, etc, this technology was applied to fabricate three dimensional (3D) nanoparticle structures in large area substrate (5 mm × 5 mm size). When voltage of EF electrode was increased, large agglomerates were eliminated and the size of particles was decreased, so well-patterned nanostructures were fabricated.

Furthermore, large amounts of charged particles could be obtained by controlling the electric field. Their number and volume concentration increased according to electric potential in low voltage area. Also this post spark discharge manipulator can be utilized to high frequency spark discharge process because of low gas flow rate condition.

Abstract (in Korean)

스파크 방전후의 플라즈마의 거동 조절을 통한 하전 나노입자의 발생

서울대학교 대학원 기계항공공학부

김 웅 식

요약

스파크 방전 법은 기상상태에서 나노 입자를 생성하는 유용한 방법이다. 이 방법은 나노입자 합성, 광학 장치, 나노 입자 어셈블리 분야 등 다양한 연구 분야에 사용되어왔다.

스파크 방전법에는 많은 장점도 있지만, 입자간 응집을 방지하고 하전 입자를 대량으로 생성하는, 극복해야 할 두 가지 과제가 있다. 지금까지 많은 연구 그룹이 이러한 과제를 극복하려고 시도해왔다. 그러나 지금까지 수행된 연구는 스파크 주파수, 스파크 에너지, 가스 유량, 이온 주입 등의 스파크 발생 전의 변수만을 조절하였기 때문에 두 가지 과제를 해결하는 데 한계가 있었다.

스파크 방전 직후 단계의 변수를 조절하는 것에 대해서는 거의 연구되어 있지 않지만, 이 연구는 스파크 방전 직후 단계의 메커니즘을 분석함으로써 이 문제점들을 근본적으로 해결하는 것이 가능하기 때문에 매우 중요하다.

본 연구에서는 입자간 응집을 방지하고 대량의 하전 입자를

발생시키기 위해 스파크 방전 직후의 영역을 전기장을 이용하여 제어할 수 있는 PSDM(post spark discharge manipulator)을 설계하고 시험했다.

또한 스파크 방전 직후 존재하는 플라즈마에 가해지는 힘을 분석함으로써 스파크 방전 후 영역에 전기장이 미치는 영향을 고찰하였고 메커니즘을 제시하였다.

본 연구는 스파크 방전에 의해 생성된 잔류 플라즈마 상의 1가 하전을 띄는 나노입자에 비균일 외부 전기장이 가해졌을때의 크기 선택 효과에 대해 보고하고 있다.

연구 결과, 가해진 전기장은 플라즈마 작은 입자들은 클라우드 밖으로 내보내어 작은 입자들이 플라즈마 안에 머물러서 중화되거나 뭉치는 것을 방지함으로써 입자의 크기분포에 영향을 주었다. 반면 플라즈마에 갇혀서 플라즈마와 함께 이동한 큰 입자는 중화되거나 벽에 부딪혀서 소멸하기 때문에 입자 크기 분포 함수는 작은 방향으로 이동한다.

본 논문에서는 전기장 효과를 설명하는 간단한 이론이 제시되었고 패터닝 기술에의 응용과 결과를 보여주었다.

주요어 : 스파크 방전, 스파크 방전 후 영역 조절기 (PSDM), 전형적인 스파크 발생기 (CSDG), 스파크 방전 후 잔류 플라즈마, 스파크 방전 전 영역, 전기력, 이온 항력, 쌍극자 매개 변수 'P'

학 번: 2009-30162